Seeing Through the ETF: Indicative NAV and Commodity Volatility Transmission

Simon-Pierre Boucher* Marie-Hélène Gagnon† Gabriel J. Power‡

July 31, 2026

Abstract

This paper builds a novel dataset of indicative Net Asset Value (iNAV) observations for commodity ETFs and measures volatility transmission between ETFs and their underlying baskets using high-frequency realized variance. Applying this design to crude oil, gold, silver, and natural gas, we show that the iNAV provides a sharper image of the volatility relationship. Decomposing realized variance into continuous and jump components, we establish that transmission runs primarily through jumps rather than diffusion, a channel that standard volatility connectedness measures may obscure. Sampling frequency also matters: 1-minute data reveal daily volatility transmission up to twice as large as 30-minute estimates. Finally, transmission differs across commodity types. For gold and silver, it is unidirectional from iNAV to ETF, consistent with passive arbitrage. For energy ETFs, which are more liquid and hold futures as underlying assets, transmission is bidirectional and asymmetric.

Keywords: ETF, volatility, transmission, commodity markets, futures, intraday, realized variance, jump, HAR, arbitrage, microstructure.
JEL Classification: G12, G13, G14, C32

*PhD student in finance, Université Laval, Quebec City QC Canada G1V 0A6, email: simon-pierre.boucher.1@ulaval.ca

†Professor of Finance and Research Fellow, CRREP, Université Laval, email: marie-helene.gagnon@fsa.ulaval.ca

‡IG Wealth Management Chairholder, Professor of Finance and Research Fellow, CRREP and CRIB, Université Laval, email: gabriel.power@fsa.ulaval.ca

1 Introduction

The exchange-traded fund (ETF) market has grown rapidly over the past two decades, with global assets under management (AUM) exceeding $23 trillion as of May 2026. The growth in the ETF market has also altered the structure of underlying asset markets (Petäjistö, 2017). ETF ownership has been found to increase non-fundamental volatility in underlying equities (Ben-David et al., 2018), weaken the link between prices and fundamentals (Israeli et al., 2017), and strengthen correlations during periods of market stress (Da and Shive, 2018). The number and economic size of commodity ETFs, such as the SPDR Gold Trust (GLD), has rapidly grown in recent years. These products offer exposure to commodity markets without the need for direct futures trading or physical storage (Gorton and Rouwenhorst, 2006), thus increasing the participation of financial investors, creating new economic links between commodity and equity prices, and establishing the ETF as an alternative venue for price discovery (Basak and Pavlova, 2016; Buyuksahin and Robe, 2014).

Commodities offer a particularly interesting setting to study ETF pricing and volatility transmission. Exchange-traded funds are usually studied as near-transparent wrappers around their holdings. For example, VOO and IVV replicate the U.S. S&P 500 market index and hold the stocks that comprise this index according to their weights. For a typical equity ETF this framing is close to exact. The underlying securities trade on the same exchanges during the same hours, and creation-redemption arbitrage pins the fund's price to its net asset value quickly and in essentially one direction. Thus, for an equity ETF, asking whether the ETF leads the basket would be similar to asking whether a shadow leads the object that casts it. In contrast, commodity ETFs break this identity in a way that is not feasible in other major ETF classes. This is because their underlying may not be the physical good, but could be instead a derivative claim. For instance, if it is a futures position in crude oil or natural gas, there are economic implications for cost-of-carry, roll, and the shape of the term structure. In the case of a stored physical claim in gold and silver there is lease-and-storage economics to consider.

Thus, for commodity ETFs, the arbitrage relationship is not as simple as it is for equities or bonds, and volatility transmission becomes a genuine economic question rather than a purely mechanical one. To the point of this paper, it is important to investigate the fund's indicative net asset value (iNAV), which is the real-time fair value of that basket. Commodity ETFs also play a role in the financialization debate (Basak and Pavlova, 2016), as they are popular retail-accessible instruments. It is important for investors, traders, hedgers and policymakers to understand how volatility travels between these vehicles and their underlyings. The direction of this volatility flow is not clear a priori. Indeed, commodity ETFs differ along another significant dimension, namely that unlike equities, in commodities the ETF may well be more liquid and more continuously accessible than its underlying. This feature provides a clear reason why the ETF might contribute to price discovery rather than simply inherit it. Whether it does, however, remains an empirical question.

The theoretical foundation of ETF pricing rests on arbitrage. Authorized participants (APs) maintain price alignment through creation and redemption, buying undervalued ETFs while selling their underlying constituents, or vice versa (Ackert and Tian, 2000). Classic arbitrage theory predicts that volatility transmission would be unidirectional, flowing from the underlying constituents (NAV) to the ETF: when underlying volatility rises, arbitrageurs trade more actively to maintain alignment, which transmits volatility to the ETF. Recent evidence challenges this prediction, documenting bidirectional transmission in which ETF trading influences underlying asset volatility (Ben-David et al., 2018; Da and Shive, 2018). This outcome arises because ETFs often trade more frequently and with smaller spreads than their constituents, making the ETF a primary venue for price formation (Glosten et al., 2021; Pan and Zeng, 2016). The relative magnitude and direction of transmission therefore reveal which market dominates information discovery and whether arbitrage functions efficiently. These questions have direct implications for hedging (directional dependencies) and for regulation, e.g., as feedback effects may amplify volatility during crises (Madhavan, 2012; Petäjistö, 2017).

This paper studies how volatility is transmitted between commodity ETFs and their underlying assets using high-frequency realized variance over 2010–2023. We focus on four major single-commodity ETFs spanning two market structures: physically-backed precious metals (SPDR Gold Trust, GLD; iShares Silver Trust, SLV) and futures-based energy funds (United States Oil Fund, USO; United States Natural Gas Fund, UNG). Our central question is whether transmission is unidirectional or bidirectional, and how its direction, strength, and time horizon vary with commodity type, sampling frequency, and the continuous versus jump nature of volatility. We study volatility transmission rather than price discovery because it reveals how risk, not just information, propagates across linked markets and whether ETF arbitrage stabilizes or amplifies it—a question central to risk management and systemic-risk regulation.

The empirical literature on ETF volatility transmission is incomplete in three respects. First, it focuses on equity ETFs using daily data (Ben-David et al., 2018; Israeli et al., 2017), leaving the intraday dynamics that govern arbitrage largely unexplored. Indeed, as arbitrage operates continuously through the day, daily aggregation may obscure rapid transmission. Second, the literature has not examined how spillovers differ across commodity types, even though precious metals trade in liquid global markets with physical arbitrage while energy commodities rely on futures with rollover costs and storage constraints—features that should generate systematically different transmission. Third, it has not distinguished the roles of underlying assets versus ETFs in driving volatility, leaving open the questionwhether ETFs passively follow their constituents or actively feed back into them.

We address these gaps by constructing minute-by-minute indicative Net Asset Value (iNAV) series for the four ETFs over thirteen years spanning the European sovereign debt crisis, the 2014–2016 commodity collapse, the COVID-19 pandemic, and the subsequent inflation surge. We combine Heterogeneous Autoregressive (HAR) models that capture the long memory of realized volatility across daily, weekly, and monthly horizons (Corsi, 2009) with Bayesian Vector Autoregression (BVAR) models to accommodate time-varying dependence while avoiding overfitting (Koop, 2013). We measure realized variance from high-frequency returns (Andersen et al., 2001) and decompose it into continuous and jump components (Barndorff-Nielsen and Shephard, 2004). We separate jumps because commodity prices respond to discrete shocks—geopolitical events, supply disruptions—that may transmit through different channels than smooth price movements, with distinct consequences for tail-risk hedging. On this basis, we test four hypotheses, stated formally in Section 3: (i) whether transmission is uni- or bidirectional and varies by commodity type; (ii) whether high-frequency sampling reveals dynamics hidden in daily data; (iii) whether jumps or the continuous component dominate transmission; and (iv) whether transmission is stable over time.

Our results reveal substantial heterogeneity across commodity types and sampling frequencies. For precious metals (GLD, SLV), transmission is strongly unidirectional from iNAV to ETF, with spillover coefficients ranging from 0.42 (silver) to 0.63 (gold) at one-minute frequency and negligible reverse effects. Energy ETFs (USO, UNG) show bidirectional transmission, with the iNAV-to-ETF direction dominant for crude oil (about four to one) and the two directions comparable for natural gas. Sampling frequency matters: the daily iNAV-to-ETF spillover is up to roughly twice as large in one-minute as in thirty-minute data. Jump components dominate continuous transmission, especially for precious metals. The BVAR analysis confirms these patterns through impulse responses and variance decompositions in which underlying volatility rivals or exceeds ETF self-persistence in explaining ETF volatility.

The paper makes two contributions. Methodologically, we construct the first comprehensive high-frequency iNAV series for commodity ETFs over an extended period, enabling precise measurement of intraday arbitrage relationships that are unobservable with daily NAV data. Empirically, we document systematic differences in transmission across commodity categories and sampling frequencies, showing that market structure shapes information transmission and that empirical inference is affected by temporal aggregation. Thus, we extend the literature on ETF volatility transmission from equity to commodity markets (Ben-David et al., 2018; Israeli et al., 2017). We further connect it to the microstructure literature (Hasbrouck, 2003; Richie et al., 2008), and we contribute to research on commodity-ETF financialization (Todorov, 2024; Buyuksahin and Robe, 2014) by showing that the effects vary in systematic ways between physically-backed and futures-based ETFs. The remainder of the paper is as follows. Section 2 describes the data and the construction of high-frequency iNAV and realized-volatility series. Section 3 presents the econometric framework and states the hypotheses. Section 4 reports the empirical results. Section 5 concludes.

2 Data and Sample Construction

Our data processing approach improves on what has been previously used in the ETF volatility literature, which typically relies on daily data and may not detect high-frequency transmission channels (Ben-David et al., 2018; Israeli et al., 2017). By constructing minute-by-minute price and indicative NAV series for four commodity ETFs over thirteen years, we capture volatility dynamics at horizons not previously examined and compare volatility transmission across heterogeneous commodity market structures.

2.1 Sample Selection and Data Sources

We study four large single-commodity ETFs, each among the top funds in its category ranked by assets under management:

- **SPDR Gold Trust (GLD)** and **iShares Silver Trust (SLV)** are physically-backed precious-metals ETFs holding bullion in trust (over $50 billion and $10 billion in assets, respectively). Physical backing minimizes tracking error but creates arbitrage frictions tied to delivery, storage, and insurance.

- **United States Oil Fund (USO)** and **United States Natural Gas Fund (UNG)** are futures-based energy ETFs tracking WTI crude oil and Henry Hub natural gas through NYMEX futures. Continuous rolling of expiring contracts generates tracking errors related to contango and backwardation (Todorov, 2024), and natural gas adds extreme seasonality and storage constraints.

We select these ETFs for three reasons: high liquidity (top-five funds by assets in each category), continuous tradability over the full sample (January 2010 to January 2023) and-, most importantly, contrasting tracking mechanisms. Physically-backed ETFs (GLD, SLV) settle through physical delivery against London Bullion Market Association (LBMA) spot prices, with no rollover costs but slower arbitrage. Futures-based ETFs (USO, UNG) are arbitraged electronically against NYMEX futures, with faster settlement but involving roll costs, contango/backwardation patterns, and basis risk. Since these market structures create different frictions, transaction costs and lags, we expect them to generate different patterns of volatility transmission. We use single-commodity rather than index ETFs to avoid cross-commodity correlation effects.

Our primary data source is the Bloomberg terminal, which provides tick-by-tick trade prices, bid–ask quotes, and volume with millisecond timestamps for the ETFs and their underlying assets. We supplement this with futures contract price data from the Chicago Mercantile Exchange (CME) and spot price data from the LBMA. We begin the sample in 2010 for three reasons: By this date, the ETFs (launched 2004–2007) had plausibly reached the trading volume and market-making infrastructure needed for reliable high-frequency data and meaningful arbitrage. Moreover, starting in 2010 avoids the atypical microstructure effects during certain periods of the 2008–2009 crisis. Lastly, consistent tick-level data became available across all instruments in our sample. The resulting thirteen-year period spans the 2010–2012 European sovereign debt crisis, the 2014–2016 commodity collapse, the 2020 COVID-19 pandemic, and the 2021–2022 inflation surge, covering diverse volatility regimes.

2.2 High-Frequency Data Construction and Cleaning

High-frequency data require careful filtering to remove microstructure noise. Starting from raw tick data over regular U.S. market hours (9:30 AM–4:00 PM EST), we apply standard procedures adapted to the ETF market structure (Barndorff-Nielsen et al., 2009). First, we remove outliers using the Brownlees and Gallo (2006) method, deleting observations more than 10 standard deviations from a rolling 20-minute median (about 0.03% of observations). Second, we apply the duration filter suggested by Hansen and Lunde (2005), excluding trades separated by more than 30 minutes, which typically indicates closures or technical failures (less than 0.1% of observations). We then build synchronized price series at 1-, 5-, and 30-minute frequencies using previous-tick interpolation (Andersen et al., 2001). The final cleaned dataset contains roughly 45 million price observations. Data loss is minimal and concentrated in thinly traded periods.

2.3 Indicative Net Asset Value (iNAV) Construction

Official NAV is published only at the end of each trading day (Petäjistö, 2017). This variable cannot capture the intraday arbitrage activities that actually drive ETF pricing. We therefore construct an indicative NAV (iNAV) at a high frequency, which provides a real-time estimate of fundamental value from current underlying prices. This approach lets us measure arbitrage and transmission at the frequency where authorized participants make creation/redemption decisions, and let us separate fundamental ETF volatility (changes in underlying value) from non-fundamental volatility (liquidity shocks, inventory effects, or temporary arbitrage breakdowns).

For physically-backed ETFs (GLD, SLV), iNAV follows a composition-based approach:

$$\text{iNAV}_t = \frac{1}{N_t}\left[\text{Cash}_t + \sum_i \left(P_{it}\cdot f_{it}\cdot q_{it}\cdot c_{it}\right)\right] \tag{1}$$

where N_t is the number of outstanding ETF shares, Cash_t is the fund's cash holdings, P_{it} is the price of underlying asset i in local currency, f_{it} the currency conversion factor, q_{it} the quantity held, and c_{it} an adjustment for accrued interest, dividends, or other cash flows. We use LBMA gold and silver prices converted to U.S. dollars at real-time exchange rates. Physical holdings are updated daily with creation/redemption activity, while intraday changes reflect only price movements.

For futures-based ETFs (USO, UNG), iNAV follows a futures-position model:

$$\text{iNAV}_t = \frac{1}{N_t}\left[\text{Cash}_t + \sum_j \left(F_{jt}\cdot cc_{jt}\cdot q_{jt}\cdot m_{jt}\right)\right]\cdot FX_t \tag{2}$$

where F_{jt} is the price of futures contract j, cc_{jt} the contract conversion factor, q_{jt} the number of contracts held, m_{jt} the contract multiplier, and FX_t any currency conversion. We use real-time NYMEX WTI crude oil and Henry Hub natural gas futures, accounting for the funds' actual contract positions and monthly roll schedules.

A technical consideration is the mismatch between ETF trading hours and underlying market hours: gold and silver trade nearly around the clock in London and Asia, while energy futures have defined sessions. To handle this issue, we weight each market session by its share of price discovery and carry forward the most recent adjusted prices when an underlying market is closed. We validate the construction against published end-of-day NAV. We find that our iNAV has a correlation greater than 0.999 with the official NAV, and mean absolute deviations of less than 5 basis points.

2.4 Realized Variance Construction and Jump Detection

We measure volatility using realized variance, i.e., the sum of squared intraday returns (Andersen et al., 2001). For asset i on day t:

$$RV_{i,t} = \sum_{j=1}^{M} r_{i,t,j}^2 \quad (3)$$

where $r_{i,t,j} = \log(P_{i,t,j}) - \log(P_{i,t,j-1})$ and M is the number of intraday returns, giving $M = 390$ (1-minute), $M = 78$ (5-minute), and $M = 13$ (30-minute). Under standard conditions, realized variance converges to integrated variance as sampling intensifies (Barndorff-Nielsen and Shephard, 2002). The choice of frequency trades statistical efficiency against microstructure bias from bid–ask bounce (Hansen and Lunde, 2005; Liu et al., 2015), so we use three frequencies to assess robustness.

To separate continuous movements from discrete jumps, we use the bipower variation (Barndorff-Nielsen and Shephard, 2004):

$$BV_{i,t} = \mu_1^{-2} \sum_{j=2}^{M} |r_{i,t,j}| \cdot |r_{i,t,j-1}| \quad (4)$$

where $\mu_1 = \sqrt{2/\pi} \approx 0.798$. Bipower variation consistently estimates integrated variance even in the presence of jumps. The jump component is

$$J_{i,t} = \max(RV_{i,t} - BV_{i,t}, 0) \quad (5)$$

and the continuous component is $C_{i,t} = RV_{i,t} - J_{i,t}$ (Huang and Tauchen, 2005). This continuous component is reported as quadratic power variation (QPV) in the estimation tables. Separating the two matters because jumps—from supply disruptions or geopolitical events—may transmit across markets differently than smooth volatility.

2.5 Descriptive Statistics and Stylized Facts

Tables 1, 2, and 3 report descriptive statistics for realized variance, bipower variation, and jumps across the three frequencies. Several stylized facts emerge. Realized variance is heterogeneous across commodities and between ETFs and their iNAVs. Natural gas and crude oil have the highest average volatility: the 5-minute mean realized variance is 0.104%, and 0.081% for the iNAV. For crude oil, the iNAV (0.081%) is more volatile than the ETF value (0.066%), as expected from the damping effect of arbitrage. The heaviest distributional tails occur in crude oil and gold: For crude oil, the iNAV realized variance reaches a maximum above 40%. For gold, the ETF series shows occasional extreme outliers (maximum near 79%), reflecting occasional disruptions in physical gold arbitrage adjustments. Precious metals are otherwise less volatile on average than energy, though for gold the ETF mean volatility (0.034%) exceeds its iNAV mean (0.012%). Jump activity is most pronounced for crude oil, consistent with this commodity's sensitivity to geopolitical and supply shocks, and it is weakest for precious metals, for which prices move more smoothly.

Figures 1, 2, 3, and 4 show the evolution of realized variance over time. All series show strong volatility clustering, which is most pronounced during the 2014–2016 oil collapse, the 2016 Brexit referendum (precious metals), and the 2020 pandemic (for all commodities). ETF–iNAV synchronization is high for precious metals but more variable for energy commodities, where periods of close co-movement alternate with divergence. As these relationships are time-varying, a simple correlation analysis would fail to detect economically significant dynamics, which motivates the modeling framework in Section 3.

Finally, all realized-variance series are stationary in both levels and logs (augmented Dickey–Fuller tests), and we validate the GLD iNAV against the NYSE indicative optimized portfolio value (IOPV), obtaining correlations above 0.995. Tests for structural breaks and the full set of robustness checks are reported with the econometric framework in Section 3.

3 Econometric Methodology

We analyze volatility transmission between commodity ETFs and their iNAVs with two complementary frameworks. Heterogeneous Autoregressive (HAR) models (Corsi, 2009) capture the long memory of realized volatility across daily, weekly, and monthly horizons and, in cross-market form, yield interpretable spillover coefficients. Bayesian Vector Autoregression (BVAR) models (Koop, 2013; Carriero et al., 2009) treat ETF and iNAV volatility as jointly endogenous, using Minnesota-prior shrinkage to control parameter proliferation and providing impulse responses and variance decompositions with proper uncertainty bands. We favor realized-variance models over GARCH because realized variance is a nearly model-free volatility estimate that forecasts better (Andersen et al., 2001), and HAR over fractionally integrated (ARFIMA) specifications because it captures long memory parsimoniously through a horizon cascade (Corsi, 2009).

3.1 Theoretical Framework for Volatility Transmission

Under frictionless arbitrage, ETF prices equal their NAV and volatility transmission is instantaneous and bidirectional (Ackert and Tian, 2000; Petäjistö, 2017). Real-world frictions—transaction costs, inventory and funding constraints—can instead create asymmetric transmission that varies across horizons and market conditions. We study volatility transmission rather than price discovery because it reveals how risk propagates and whether arbitrage stabilizes or amplifies fluctuations, with direct implications for hedging effectiveness and systemic risk. Examining multiple horizons follows the heterogeneous market hypothesis (Müller et al., 1997), under which day traders, institutions, and longer-horizon participants generate volatility that persists over their characteristic time scales. Finally, the contrast between physically-backed ETFs (GLD, SLV), whose arbitrage requires physical delivery, and futures-based ETFs (USO, UNG), which face roll costs and basis risk (Todorov, 2024), motivates our cross-sectional comparison.

3.2 Heterogeneous Autoregressive (HAR) Models

The HAR model (Corsi, 2009) is the dominant framework for realized-volatility dynamics (Andersen et al., 2007). The baseline specification is

$$\log(RV_{i,t}) = \beta_0 + \beta_1 \log(RV_{i,t-1}) + \beta_2 \log(\overline{RV}_{i,t-5:t-1}) + \beta_3 \log(\overline{RV}_{i,t-22:t-1}) + \varepsilon_{i,t} \tag{6}$$

where $\overline{RV}_{i,t-h:t-1} = \frac{1}{h}\sum_{j=1}^{h} RV_{i,t-j}$ averages realized variance over the previous h days, capturing daily, weekly ($h = 5$), and monthly ($h = 22$) persistence. The log transform keeps fitted volatility positive and stabilizes the residual variance.

To measure transmission, we add cross-market terms. For iNAV volatility,

$$\begin{aligned}\log(RV_{t,\mathrm{NAV}}) = \beta_0 + \beta_1 \log(RV_{t-1,\mathrm{NAV}}) + \beta_2 \log(\overline{RV}_{t-5:t-1,\mathrm{NAV}}) + \beta_3 \log(\overline{RV}_{t-22:t-1,\mathrm{NAV}}) \\ + \alpha_1 \log(RV_{t-1,\mathrm{ETF}}) + \varepsilon_{t,\mathrm{NAV}}\end{aligned} \tag{7}$$

and symmetrically for ETF volatility,

$$\begin{aligned}\log(RV_{t,\mathrm{ETF}}) = \gamma_0 + \gamma_1 \log(RV_{t-1,\mathrm{ETF}}) + \gamma_2 \log(\overline{RV}_{t-5:t-1,\mathrm{ETF}}) + \gamma_3 \log(\overline{RV}_{t-22:t-1,\mathrm{ETF}}) \\ + \delta_1 \log(RV_{t-1,\mathrm{NAV}}) + \varepsilon_{t,\mathrm{ETF}}\end{aligned} \tag{8}$$

Each equation includes the own daily, weekly, and monthly terms and a single cross-market term at the daily lag, following the parsimony of the HAR cascade. The coefficient α_1 measures the daily ETF-to-iNAV spillover and δ_1 the daily iNAV-to-ETF spillover; the own weekly (β_2, γ_2) and monthly (β_3, γ_3) terms capture longer-horizon volatility persistence.

To separate the transmission of continuous and jump volatility, we estimate a HAR-CJ-X specification using the components C and J defined in Section 2:

$$\begin{aligned} \log(RV_{t,\text{NAV}}) = \beta_0 + \beta_1 \log(C_{t-1,\text{NAV}}) + \beta_2 \log(\overline{C}_{t-5:t-1,\text{NAV}}) + \beta_3 \log(\overline{C}_{t-22:t-1,\text{NAV}}) \\ + \beta_4 \log(1 + J_{t-1,\text{NAV}}) + \beta_5 \log(1 + \bar{J}_{t-5:t-1,\text{NAV}}) + \beta_6 \log(1 + \bar{J}_{t-22:t-1,\text{NAV}}) \\ + \alpha_1 \log(C_{t-1,\text{ETF}}) + \alpha_2 \log(1 + J_{t-1,\text{ETF}}) + \varepsilon_{t,\text{NAV}} \end{aligned} \tag{9}$$

with an analogous ETF equation. The own continuous and jump components enter at all three horizons through β_1–β_3 and β_4–β_6; the daily cross-market continuous and jump spillovers are α_1 and α_2. The transform $\log(1 + J_t)$ keeps jump terms defined when $J_t = 0$.

3.3 Bayesian Vector Autoregression (BVAR)

The HAR cascade imposes a fixed horizon structure. As a flexible complement, we estimate a VAR treating ETF and iNAV volatility as jointly endogenous:

$$\mathbf{y}_t = \mathbf{c} + \sum_{k=1}^{p} \mathbf{A}_k \mathbf{y}_{t-k} + \mathbf{u}_t \tag{10}$$

where $\mathbf{y}_t = [\log(RV_{t,\text{ETF}}), \log(RV_{t,\text{NAV}})]'$ and $\mathbf{u}_t \sim \mathcal{N}(\mathbf{0}, \boldsymbol{\Sigma})$. Information criteria (BIC) select $p = 2$. Because unrestricted VARs over-parameterize, we apply the Minnesota prior (Litterman, 1986):

$$
\begin{aligned}
\beta_{ij}^{(k)} &\sim \mathcal{N}(0, \lambda_1^2 \cdot k^{-\lambda_3}) \quad \text{for } i \neq j \\
\beta_{ii}^{(1)} &\sim \mathcal{N}(1, \lambda_1^2) \\
\beta_{ii}^{(k)} &\sim \mathcal{N}(0, \lambda_1^2 \cdot k^{-\lambda_3}) \quad \text{for } k > 1
\end{aligned}
\tag{11}
$$

where $\beta_{ij}^{(k)}$ is the coefficient on variable j at lag k in equation i; λ_1 controls overall tightness, λ_2 cross-variable shrinkage, and λ_3 lag decay. We set $\lambda_1 = 0.2$, $\lambda_2 = 0.5$, $\lambda_3 = 2$ and vary them in sensitivity analysis. The prior encodes that own lags matter more than others, recent lags more than distant ones, and coefficients are not extreme—assumptions well suited to persistent, mean-reverting volatility.

We estimate by Gibbs sampling, alternating between the coefficients (multivariate normal given $\mathbf{\Sigma}$) and the covariance (inverse-Wishart given the coefficients):

$$
\boldsymbol{\beta} | \mathbf{\Sigma}, \mathbf{Y} \sim \mathcal{N}(\hat{\boldsymbol{\beta}}, \mathbf{\Sigma} \otimes (\mathbf{X}'\mathbf{X} + \mathbf{V}_0^{-1})^{-1}), \qquad \hat{\boldsymbol{\beta}} = (\mathbf{X}'\mathbf{X} + \mathbf{V}_0^{-1})^{-1}(\mathbf{X}'\text{vec}(\mathbf{Y}) + \mathbf{V}_0^{-1}\boldsymbol{\beta}_0) \tag{12}
$$

$$
\mathbf{\Sigma} | \boldsymbol{\beta}, \mathbf{Y} \sim \text{IW}(\mathbf{S} + \mathbf{S}_0, T + \nu_0) \tag{13}
$$

where $\mathbf{Y}$ and $\mathbf{X}$ are the stacked data, $\mathbf{V}_0$, $\mathbf{S}_0$, and ν_0 are prior parameters, $\mathbf{S}$ the residual sum of squares, and T the sample size. We run 50,000 iterations, discard 10,000 as burn-in, and thin every tenth draw; convergence is assessed with trace plots and the Geweke test.

From the posterior we compute orthogonalized impulse responses and forecast error variance decompositions:

$$
\text{IRF}(h) = \mathbf{C}_h \mathbf{P}, \qquad \text{FEVD}_{i,j}(h) = \frac{\sum_{k=0}^{h-1} [\mathbf{C}_k \mathbf{P}]_{i,j}^2}{\sum_{k=0}^{h-1} [\mathbf{C}_k \mathbf{\Sigma} \mathbf{C}_k']_{i,i}} \tag{14}
$$

where $\mathbf{C}_h$ is the h-step moving-average matrix and $\mathbf{P}$ the Cholesky factor of $\mathbf{\Sigma}$. We order iNAV before ETF, so iNAV innovations may affect ETF volatility contemporaneously but not the reverse, reflecting that underlying price movements lead ETF adjustments through arbitrage. The confidence bands follow Sims and Zha (1999). A high $\text{FEVD}_{\text{ETF,NAV}}(h)$ indicates that iNAV innovations explain ETF volatility, and conversely for $\text{FEVD}_{\text{NAV,ETF}}(h)$.

3.4 Hypotheses and Testing

We test four hypotheses, mapping each to coefficients in the equations above.

H1 (Direction and cross-commodity heterogeneity). Theory predicts unidirectional iNAV-to-ETF transmission, but a more liquid ETF can reverse the flow (Glosten et al., 2021). We expect physically-backed precious metals to show unidirectional iNAV-to-ETF transmission and futures-based energy ETFs more balanced bidirectional transmission. In equations (7)–(8), ETF-to-iNAV transmission tests $H_0 : \alpha_1 = 0$ against $H_a : \alpha_1 \neq 0$, and iNAV-to-ETF transmission tests $H_0 : \delta_1 = 0$ against $H_a : \delta_1 \neq 0$. Transmission is unidirectional when only δ_1 is significant and bidirectional when both α_1 and δ_1 are significant. Heterogeneity means these outcomes differ across commodities.

H2 (Frequency dependence). If arbitrage occurs within minutes, daily aggregation would understate transmission. Using the daily spillover coefficients δ_1 and α_1 estimated at the 1-, 5-, and 30-minute frequencies, we test $H_0 : \delta_1^{(1m)} = \delta_1^{(5m)} = \delta_1^{(30m)}$ against H_a : the coefficients differ across frequencies.

H3 (Jumps versus continuous component). Tail risk from discrete shocks is harder to hedge than smooth volatility, which is why we decompose volatility into continuous and jump parts. In the HAR-CJ-X model (9), we compare the daily cross-market jump and continuous spillovers, testing $H_0 : \alpha_2 = \alpha_1$ (jump and continuous transmission equal) against $H_a : \alpha_2 > \alpha_1$ (jump transmission dominates), and analogously for the ETF equation.

H4 (Stability over time). Over a data sample spanning several crises, patterns of transmission may evolve. We re-estimate the BVAR over sub-periods (2010–2014, 2015–2019, 2020–2023) and apply the structural-break test of Bai and Perron (2003), testing H_0 : transmission coefficients are constant across regimes against H_a : they change.

3.5 Estimation, Model Selection, and Robustness

We select lag lengths and compare nested models with the AIC and BIC (the DIC for Bayesian models, which accounts for shrinkage), and evaluate out-of-sample forecasts with rolling windows (a 1,000-day estimation window re-estimated every 250 days) at the 1-, 5-, and 22-day horizons using RMSE and MAE. Residual diagnostics include the Ljung–Box (serial correlation), Breusch–Pagan (heteroskedasticity), and Jarque–Bera (normality) tests, plus posterior predictive checks for the BVAR. We also gauge economic magnitude through the effect of one-standard-deviation shocks on forecast volatility.

We assess robustness along three dimensions, consolidating the checks noted in Section 2. First, *specifications*: alternative HAR lag structures, BVAR lags from one to four, level and square-root (rather than log) transforms, and time-varying-parameter versions. Second, *sample stability*: the sub-period and regime estimation underlying H4, structural-break tests (Bai and Perron, 2003)—which flag the 2014 oil collapse, the 2016 Brexit referendum, and the 2020 pandemic—and bootstrap inference. Our transmission results hold across regimes, indicating they capture general mechanisms rather than period-specific effects. Third, *data construction*: additional 15- and 60-minute frequencies, alternative estimators (truncated realized variance, realized kernels, range-based measures), and alternative iNAV constructions (currency conversion, cash treatment), including validation against the GLD IOPV. Our main findings are robust throughout.

4 Empirical Results

This section reports the results of our empirical analysis of volatility transmission between commodity ETFs and their underlying assets. We organize the presentation of results around the four hypotheses stated in Section 3, analyzing them in order: namely, the direction of transmission and its variation across commodity types (H1), the role of sampling frequency (H2), the relative importance of jump and continuous components (H3), and the stability of transmission over time (H4).

4.1 Direction of Transmission and Commodity-Specific Asymmetries

Our first hypothesis concerns whether transmission between an ETF and its iNAV is unidirectional or bidirectional, and whether this varies across commodities (H1). As discussed in Section 3, theory predicts a flow only from iNAV to ETF, but a more liquid ETF can reverse the direction of the flow. In the case of commodities, the storability and settlement mechanism is also expected to matter. We therefore expect physically-backed precious metals to show unidirectional iNAV-to-ETF transmission, and futures-based energy ETFs more balanced bidirectional transmission.

The HAR-X estimates in Tables 4 through 6 reject the null of uniform bidirectional transmission across all commodities, extending the heterogeneity documented by Gorton and Rouwenhorst (2006) and Buyuksahin and Robe (2014) to the ETF setting and consistent with Basak and Pavlova (2016) on how financialization effects vary across commodity types.

The results for precious metals show a strongly unidirectional transmission from iNAV to ETF, with little evidence of reverse transmission. Consider the iNAV-to-ETF coefficient, which is the coefficient for lagged NAV volatility in the ETF equation. For gold at a 1-minute frequency, this coefficient is 0.632 (Table 5), which is among the largest across commodities, while the ETF-to-iNAV effect (i.e., lagged ETF volatility in the NAV equation) is not statistically different from zero (-0.001, $p = 0.96$). The results for silver show a similar but weaker pattern: the NAV-to-ETF coefficient is 0.418 while the reverse effect is 0.004 and not significant. On the other hand, our results for energy commodities show bidirectional transmission. For crude oil at a 1-minute frequency, the iNAV-to-ETF coefficient is 0.378 and the ETF-to-iNAV coefficient is 0.089. Both are significant at the 1% level, and the coefficient for iNAV-to-ETF is roughly four times larger. The results for natural gas are the most directionally balanced: the effects in both directions are significant and of similar magnitude (iNAV-to-ETF 0.079; ETF-to-iNAV 0.127). This contrast between the strongly unidirectional results for metals and the bidirectional results for energy supports our hypothesis H1. Indeed, the evidence confirms that physical versus futures-based arbitrage, settlement mechanism, and liquidity shape the transmission of volatility between the commodity underlying and the ETF.

These patterns are confirmed by the results for the formal tests described in Section 3. The ETF-to-iNAV restriction $H_0 : \alpha_1 = 0$ in equation (7) is not rejected for gold or silver—their reverse coefficients are insignificant at every frequency—but is rejected at the 1% level for crude oil and natural gas. The iNAV-to-ETF restriction $H_0 : \delta_1 = 0$ in equation (8) is rejected at the 1% level for all four commodities. Transmission is therefore unidirectional (iNAV-to-ETF) for precious metals and bidirectional for energy. Moreover, the iNAV-to-ETF channel dominates for crude oil (with a magnitude of about four to one), while for natural gas the effects for the two directions are comparable.

The economic interpretation is consistent across models. In precious metals, arbitrage requires physical delivery against LBMA bullion, which is costly and slow. Authorized participants readily create or redeem ETF shares in response to underlying price moves, but cannot easily push ETF-specific shocks back into the tightly arbitraged spot market, so volatility flows essentially one way. The reverse coefficients for both metals hover near zero at all frequencies, confirming that ETF activity does not transmit volatility back to the spot market. In energy markets, by contrast, both the ETF and the underlying futures settle electronically and trade with comparable liquidity, so shocks propagate in both directions, even though fundamental supply-and-demand information still enters first through the futures-based iNAV.

Within precious metals, gold shows stronger unidirectional effects than silver at every frequency. The iNAV-to-ETF coefficients are 0.632 at a 1-minute and 0.387 at a 30-minute frequency for gold, versus 0.418 to 0.277 for silver. These results are consistent with the hypothesis that gold is a financial store of value, while silver carries additional industrial demand-related volatility. The reverse (ETF-to-iNAV) coefficients for both metals stay close to zero across frequencies: gold between -0.015 and 0.021, silver between -0.034 and 0.004, and neither is economically meaningful. In the category of energy commodities, crude oil shows a clear iNAV-to-ETF dominance across frequencies. However, the effects are more balanced for natural gas. For iNAV-to-ETF and ETF-to-iNAV, respectively, the coefficients are 0.105 and 0.126 at the 5-minute, and 0.081 and 0.074 at the 30-minute frequency. These results reflect the illiquidity, storage limits, and contango that impede arbitrage in the ETF and futures markets.

As the HAR-X specification includes cross-market terms only at the daily lag, directional transmission is identified at the daily horizon. The weekly and monthly coefficients measure each series' own persistence rather than spillovers. This own-persistence is high and, for precious metals, stable across horizons and frequencies: for instance, gold's weekly own-volatility coefficient stays near 0.33, confirming the presence of long memory in realized volatility.

4.2 The Relevance of Using High-Frequency Data

Our second hypothesis (H2) is that higher-frequency sampling reveals transmission that is obscured in daily data. Tables 4, 5, and 6 report the HAR-X estimates at 5-, 1-, and 30-minute frequencies. The daily iNAV-to-ETF transmission is markedly larger at a finer sampling frequency. For crude oil, it is measured at 0.378 at a 1-minute, 0.311 at a 5-

minute, and 0.20 at a 30-minute frequency. The 1-minute estimate represents a 22% increase over the 5-minute estimate and nearly double the 30-minute estimate. Thus, much of the same-day arbitrage transmission occurs within minutes, and measurements of this mechanism would be understated at a coarser sampling, as is traditionally used in the literature.

The sensitivity of estimates according to frequency also varies by commodity. The iNAV-to-ETF transmission decreases substantially from 1-minute to 30-minute sampling in the case of crude oil (0.378 to 0.20, i.e., a 47% drop), gold (0.632 to 0.387, or 39% smaller), and silver (0.418 to 0.277, or 34% smaller). It is, however, essentially flat for natural gas (0.079 versus 0.081). The economic interpretation is that transmission in the actively and continuously arbitraged crude oil and bullion markets clears within minutes, while for natural gas this adjusts over longer horizons because storage and pipeline constraints slow down the arbitrage activities that would otherwise help equalize ETF and underlying volatility.

The reverse channel, ETF-to-iNAV transmission, is empirically weaker. Moreover, unlike the iNAV-to-ETF channel, the estimated effects do not strengthen monotonically with the sampling frequency. For crude oil, the daily ETF-to-iNAV coefficient is 0.089 at a 1-minute, 0.111 at a 5-minute, and 0.103 at a 30-minute frequency, peaking at the intermediate horizon rather than rising with the frequency. The contrast between the strongly frequency-dependent iNAV-to-ETF channel and this flatter reverse channel reinforces the directional dominance finding which we describe under hypothesis H1.

Overall, we reject the null hypothesis of frequency-invariant transmission. A Wald test of $H_0 : \delta_1^{(1m)} = \delta_1^{(5m)} = \delta_1^{(30m)}$ on the daily iNAV-to-ETF coefficient rejects equality at the 1% level for crude oil, gold, and silver; for natural gas, whose spillover is small and flat across frequencies, the difference is not significant. Daily data thus understate short-horizon transmission by up to roughly a factor of two for the most affected commodities, which would lead to incorrect conclusions about arbitrage effectiveness, addressing the sampling-frequency question raised by Hansen and Lunde (2005). For practitioners, this finding supports the relevance of high-frequency market monitoring to detect transmission patterns that are understated in daily analysis.

4.3 Jump Components and Discontinuous Volatility Transmission

Our third hypothesis (H3) concerns whether transmission is driven by the continuous (diffusion) component or by jumps. Tables 7, 8, and 9 report the HAR-CJ-X model estimates. Across the four commodities, the daily cross-market jump coefficient dwarfs the continuous one: discrete price moves transmit volatility, while smooth price moves essentially do not. In the dominant iNAV-to-ETF direction at a 1-minute frequency, the jump transmission (lagged NAV jump in the ETF equation) is large and positive—0.892 for gold, 0.578 for silver, 0.432 for crude oil, 0.09 for natural gas—while the corresponding continuous transmission is near zero or negative for every commodity (gold −0.123, silver −0.065, crude oil −0.019, natural gas −0.002). The effect is strongest for precious metals, where the jump component is the largest in the sample.

The same pattern holds in the reverse (ETF-to-iNAV) direction but with smaller economic magnitudes: the daily jump coefficient is 0.096 for crude oil and 0.128 for natural gas, while the continuous coefficients are near −0.01. Natural gas shows the weakest iNAV-to-ETF jump coefficient (0.090), which is consistent with natural gas volatility spikes arising from idiosyncratic, localized events—hurricanes, pipeline failures, extreme weather—that do not propagate systematically. In contrast, there is a larger value for the *own* continuous effect: i.e., the weekly own-continuous coefficient reaches 0.116 at 1-minute frequency. This result suggests a separate, within-market phenomenon rather than a cross-market transmission pattern. Testing $H_0 : \alpha_2 = \alpha_1$ (daily jump versus continuous effect) against $H_a : \alpha_2 > \alpha_1$, we find that the dominance of the jump component is confirmed at the 1% level for all four commodities. This result supports H3: transmission mainly occurs through discrete jumps rather than continuous diffusion, which has implications for tail-risk hedging. Indeed, jump-driven volatility is harder to hedge with strategies that are usually built for the assumption of continuous price processes and volatility diffusions.

4.4 Bayesian VAR Analysis and Stability Over Time

Our fourth hypothesis (H4) concerns whether transmission is stable over time. The BVAR results shown in Tables 10–13 characterize the joint dynamics of ETF and iNAV volatility and, through sub-period estimation, the stability of the coefficient estimates. Since the BVAR treats the two volatilities as endogenous, it further provides a check on the HAR-X spillover coefficients without imposing a cascade structure. Across the four commodities, the results for the BVAR model confirm the asymmetries documented using the HAR-X model. Moreover, the cross-market coefficients remain stable across the 2010–2014, 2015–2019, and 2020–2023 sub-periods. Thus, we do not find evidence that the transmission mechanisms meaningfully change over time. The structural break test due to Bai and Perron (2003) indicates breaks in the volatility time series during the 2014 crude oil price collapse, the 2016 Brexit referendum, and the 2020 Covid-19 pandemic. However, reestimating the BVAR model for each regime period does not change the sign and relative magnitude of the cross-market coefficients. Therefore, we fail to reject the null hypothesis (H4) of a volatility transmission model that is stable over the full sample period.

For crude oil (Table 10), both volatilities are strongly persistent (iNAV first-lag coefficient 0.5704, 95% credible interval [0.5237, 0.6171]; second lag 0.2606 [0.2206, 0.3005]). The ETF has only a weak effect on the iNAV (first lag 0.0735 [0.0343, 0.1135]), whereas the iNAV strongly drives the ETF: its first-lag effect (0.2861 [0.2315, 0.3433]) is comparable to ETF self-persistence (0.2941 [0.2460, 0.3418]) and its second-lag effect remains economically large (0.1934 [0.1443, 0.2410]). That the iNAV's first-lag effect rivals the ETF's own self-persistence is striking: for crude oil, underlying volatility is about as important as the ETF's recent volatility in explaining today's ETF volatility—the BVAR counterpart of the strong iNAV-to-ETF spillover found in the HAR-X estimates.

Gold (Table 11) shows the most asymmetric configuration. The ETF has essentially no effect on the iNAV (first lag -0.0101 [-0.0547, 0.0336], with only a marginal second-lag effect of 0.0383 [0.0001, 0.0759]), while the iNAV dominates the ETF: its first-lag effect (0.3487 [0.2848, 0.4126]) exceeds ETF self-persistence (0.1549 [0.1004, 0.2083]) by more than twofold, with a large second lag (0.2758 [0.2221, 0.3307]). Silver (Table 12) is intermediate: iNAV self-persistence is the highest in the sample (first lag 0.6192 [0.5631, 0.6738]), the ETF-to-iNAV effect remains negligible (-0.0446 [-0.0932, 0.0051], turning weakly positive but still economically trivial at the second lag, 0.0584 [0.0176, 0.0996]), and the iNAV-to-ETF effect is strong (first lag 0.3760 [0.3102, 0.4404] versus ETF self-persistence 0.1790 [0.1226, 0.2362]) and remains economically large at the second lag (0.2016 [0.1471, 0.2563]). Natural gas (Table 13) shows the clearest bidirectionality. Its iNAV is moderately persistent (first lag 0.3919 [0.3488, 0.4366], second lag 0.2313 [0.1915, 0.2715]) and, unlike the other commodities, the ETF affects the iNAV through both lags, with a larger second-lag effect (0.0799 [0.0381, 0.1214] then 0.1567 [0.1189, 0.1938]), indicating that ETF activity feeds back to the underlying market through delayed channels tied to natural-gas storage operations. The forecast error variance decompositions reinforce this interpretation. Indeed, iNAV innovations explain a large and increasing share of ETF volatility forecast errors at longer horizons, while the share of iNAV forecast-error variance attributable to ETF innovations stays small for every commodity and is near zero for gold and silver. The impulse responses examined below confirm the same asymmetry.

4.5 Graphical Evidence on Volatility Patterns and Dynamic Responses

The realized volatility series shown in Figures 1–4 corroborate the findings reported above. For crude oil (Figure 1), ETF and iNAV volatility co-move closely with synchronized peaks during stress periods, consistent with bidirectional transmission. For gold (Figure 2), iNAV volatility consistently precedes ETF volatility in periods of significant spikes, which is the visual counterpart of unidirectional iNAV-to-ETF transmission. Silver (Figure 3) shows the same pattern, but with occasional divergence, while natural gas (Figure 4) shows the most frequent ETF–iNAV divergences.

The impulse responses shown in Figures 5–8 tell the same story but add evidence on how the shocks evolve over time. For crude oil (Figure 5), iNAV shocks produce large, persistent responses in ETF volatility while ETF shocks produce small, transitory responses in the iNAV. Gold (Figure 6) shows the most pronounced asymmetry, with negligible responses of the iNAV to ETF shocks. Silver (Figure 7) is similar but noisier, while natural gas (Figure 8) shows sizable responses in both directions with delayed peaks, confirming bidirectional transmission.

4.6 Summary of the Evidence for the Hypotheses

Taken together, the estimates from the HAR-X, HAR-CJ-X and BVAR models support our four research hypotheses, and the formal tests defined in Section 3 reject each null hypothesis. We can summarize as follows.

H1. We find that transmission is heterogeneous: the reverse (ETF-to-iNAV) coefficient is not significant for gold and silver but it is significant for crude oil and natural gas, while the forward (iNAV-to-ETF) coefficient is significant everywhere. Transmission is therefore unidirectional from iNAV to ETF for precious metals (a magnitude about four to one greater) and bidirectional for energy commodities (the coefficients are similar in magnitude). Thus, we reject the null hypothesis of uniform bidirectional transmission and we extend the evidence from Gorton and Rouwenhorst (2006) to setting of commodity volatility. **H2.** Transmission is frequency-dependent: the daily iNAV-to-ETF spillover is up to roughly twice as large at the 1-minute as the 30-minute frequency. It is flat only for natural gas. These results confirm that daily data understate these volatility dynamics (Hansen and Lunde, 2005; Liu et al., 2015). **H3.** The daily cross-market jump component of transmission dwarfs the continuous part for all four commodities—most sharply for precious metals (i.e., the jump coefficient for gold iNAV-to-ETF jump is 0.892 versus -0.123 for the continuous component)—so transmission occurs mainly through discrete jumps. **H4.** The cross-market coefficients are stable across sub-periods and are robust to astructural-break test, so the documented mechanisms hold in general and are not specific to sub-periods.

These findings build around a single mechanism, namely that the market structure and the arbitrage mechanism that links an ETF to its underlying asset—physical delivery for precious metals versus electronic futures settlement for energy—strongly shapes the characteristics of volatility transmission (e.g., direction, magnitude, horizon, and importance of jump vs diffusion parts), consistent with the arguments of Petäjistö (2017) and Basak and Pavlova (2016). Finally, we explainthe implications for investors, market makers, and regulators in the conclusion.

5 Conclusion

Using high-frequency realized variance and a combination of HAR and Bayesian VAR models, this paper examines volatility transmission between four commodity ETFs and their underlying assets over the period 2010–2023. We find that volatility transmission is unidirectional from iNAV to ETF for physically-backed precious metals (GLD, SLV), while it is bidirectional (though still dominated by iNAV-to-ETF effects) for futures-based energy commodity funds (USO, UNG). Short-horizon transmission is far stronger in high-frequency data than in daily data, while longer-horizon effects are frequency-invariant; jump components transmit more strongly than continuous ones across all commodities; and these patterns are stable across sub-periods.

These results show how arbitrage operates in practice and how its effectiveness depends on market structure, extending the limits-to-arbitrage frameworks of Ackert and Tian (2000), Pontiff (1996), and Gromb and Vayanos (2010). The unidirectional transmission which we document for precious metals is consistent with physical-delivery frictions that limit ETF activity from influencing underlying prices. In contrast, the more balanced volatility transmission in energy commodity markets fits the concept of futures-based arbitrage with electronic settlement, as argued by Basak and Pavlova (2016). The frequency-specific results suggest that arbitrage operates primarily through high-frequency channels. The evidence of longer-horizon persistence reflects separate fundamental forces, building on the intraday microstructure analysis of Hasbrouck (2003) and Richie et al. (2008). The dominance of jumps in the transmission of volatility, which we identify using the bipower variation decomposition due to Barndorff-Nielsen and Shephard (2004) and Huang and Tauchen (2005), indicates that models used for ETF pricing should pay separate attention to the continuous and discontinuous components of volatility.

In terms of methodology, our high-frequency iNAV series is the first that are built specifically for commodity ETFs over an extended sample period. These new series allow us to measure intraday arbitrage relationships that are unobservable when one uses end-of-day NAV (Petäjistö, 2017). Moreover, our comparison of HAR and BVAR models, together with a thorough analysis by sampling frequency, shows that temporal aggregation strongly affects the reliability of the empirical conclusions that can be drawn (Corsi, 2009; Koop, 2013; Andersen et al., 2007).

The findings in this paper carry practical implications for different market participants and extend the risk management discussion of Madhavan (2012) and Staer (2017). For investors and risk managers, we show that precious metals ETF volatility can be forecast from underlying volatility alone, while energy ETF models must account for bidirectional feedback. Both benefit from high-frequency information for short horizons. For market makers and authorized participants, arbitrage in precious metals flows mainly from underlying markets to ETFs, while energy markets contain more balanced bidirectional opportunities (Hendershott and Riordan, 2013). For regulators, the asymmetries that we document suggest monitoring that is tailored to the commodity type: precious metals markets show little ETF feedback and thus have a lower destabilization risk, while energy markets exhibit stronger bidirectional links warranting closer monitoring during stress periods (O'Hara and Zhou, 2021; Dannhauser, 2017). The strength of the jump transmission further suggests that stress testing should account for discontinuous shock scenarios.

Finally, for future work, we note that the high-frequency iNAV methodology shown in this paper could be applied to equity, international, and fixed-income ETFs where similar arbitrage mechanisms operate. Future research could also investigate the relationship between jumps, which we find drive volatility transmission, to specific news events, order-flow imbalances, and market-maker inventory constraints.

References

Ackert, L. F. and Y. S. Tian (2000). Arbitrage and valuation in the market for Standard & Poor's depositary receipts. *Financial Management 29*(3), 71–87.

Andersen, T. G., T. Bollerslev, and F. X. Diebold (2007). Roughing it up: Including jump components in the measurement, modeling, and forecasting of return volatility. *The Review of Economics and Statistics 89*(4), 701–720.

Andersen, T. G., T. Bollerslev, F. X. Diebold, and H. Ebens (2001). The distribution of realized stock return volatility. *Journal of Financial Economics 61*(1), 43–76.

Bai, J. and P. Perron (2003). Computation and analysis of multiple structural change models. *Journal of Applied Econometrics 18*(1), 1–22.

Barndorff-Nielsen, O. E., P. R. Hansen, A. Lunde, and N. Shephard (2009). Realized kernels in practice: Trades and quotes. *The Econometrics Journal 12*(3), C1–C32.

Barndorff-Nielsen, O. E. and N. Shephard (2002). Econometric analysis of realized volatility and its use in estimating stochastic volatility models. *Journal of the Royal Statistical Society: Series B 64*(2), 253–280.

Barndorff-Nielsen, O. E. and N. Shephard (2004). Power and bipower variation with stochastic volatility and jumps. *Journal of Financial Econometrics 2*(1), 1–37.

Basak, S. and A. Pavlova (2016). A model of financialization of commodities. *The Journal of Finance 71*(4), 1511–1556.

Ben-David, I., F. Franzoni, and R. Moussawi (2018). Do ETFs increase volatility? *The Journal of Finance 73*(6), 2471–2535.

Brownlees, C. T. and G. M. Gallo (2006). Financial econometric analysis at ultra-high frequency: Data handling concerns. *Computational Statistics & Data Analysis 51*(4), 2232–2245.

Buyuksahin, B. and M. A. Robe (2014). Speculation, commodities and cross-market linkages. *Journal of International Money and Finance 42*, 38–70.

Carriero, A., G. Kapetanios, and M. Marcellino (2009). Forecasting exchange rates with a large Bayesian VAR. *International Journal of Forecasting 25*(2), 400–417.

Corsi, F. (2009). A simple approximate long-memory model of realized volatility. *Journal of Financial Econometrics 7*(2), 174–196.

Da, Z. and S. Shive (2018). Exchange traded funds and asset return correlations. *European Financial Management 24*(1), 136–168.

Dannhauser, C. D. (2017). The impact of innovation: Evidence from corporate bond exchange-traded funds. *Journal of Financial Economics 125*(3), 537–560.

Glosten, L., S. Nallareddy, and Y. Zou (2021). ETF activity and informational efficiency of underlying securities. *Management Science 67*(1), 22–47.

Gorton, G. and K. G. Rouwenhorst (2006). Facts and fantasies about commodity futures. *Financial Analysts Journal 62*(2), 47–68.

Gromb, D. and D. Vayanos (2010). Limits of arbitrage: The state of the theory. *Annual Review of Financial Economics 2*, 251–275.

Hansen, P. R. and A. Lunde (2005). A realized variance for the whole day based on intermittent high-frequency data. *Journal of Financial Econometrics 3*(4), 525–554.

Hasbrouck, J. (2003). Intraday price formation in US equity index markets. *The Journal of Finance 58*(6), 2375–2400.

Hendershott, T. and R. Riordan (2013). Algorithmic trading and the market for liquidity. *Journal of Financial and Quantitative Analysis 48*(4), 1001–1024.

Huang, X. and G. Tauchen (2005). The relative contribution of jumps to total price variance. *Journal of Financial Econometrics 3*(4), 456–499.

Israeli, D., C. M. Lee, and S. A. Sridharan (2017). Is there a dark side to exchange traded funds? An information perspective. *Review of Accounting Studies 22*(3), 1048–1083.

Koop, G. (2013). Forecasting with medium and large Bayesian VARs. *Journal of Applied Econometrics 28*(2), 177–203.

Litterman, R. B. (1986). Forecasting with Bayesian vector autoregressions—five years of experience. *Journal of Business & Economic Statistics 4*(1), 25–38.

Liu, L. Y., A. J. Patton, and K. Sheppard (2015). Does anything beat 5-minute RV? A comparison of realized measures across multiple asset classes. *Journal of Econometrics 187*(1), 293–311.

Madhavan, A. (2012). Exchange-traded funds, market structure, and the flash crash. *Financial Analysts Journal 68*(4), 20–35.

Müller, U. A., M. M. Dacorogna, R. D. Davé, R. B. Olsen, O. V. Pictet, and J. E. von Weizsäcker (1997). Volatilities of different time resolutions—analyzing the dynamics of market components. *Journal of Empirical Finance 4*(2-3), 213–239.

O'Hara, M. and X. A. Zhou (2021). Anatomy of a liquidity crisis: Corporate bonds in the COVID-19 crisis. *Journal of Financial Economics 142*(1), 46–68.

Pan, K. and Y. Zeng (2016). ETF arbitrage under liquidity mismatch. *Journal of Financial Economics 120*(3), 617–635.

Petäjistö, A. (2017). Inefficiencies in the pricing of exchange-traded funds. *Financial Analysts Journal 73*(1), 24–54.

Pontiff, J. (1996). Costly arbitrage: Evidence from closed-end funds. *The Quarterly Journal of Economics 111*(4), 1135–1151.

Richie, N., R. T. Daigler, and K. C. Gleason (2008). The limits to stock index arbitrage: Examining S&P 500 futures and SPDRs. *Journal of Futures Markets 28*(12), 1182–1205.

Sims, C. A. and T. Zha (1999). Error bands for impulse responses. *Econometrica 67*(5), 1113–1155.

Staer, A. (2017). Asset management via ETFs. *The Review of Financial Studies 30*(9), 3225–3264.

Todorov, K. (2024). When passive funds affect prices: Evidence from volatility and commodity ETFs. *Review of Finance 28*(3), 831–863.

6 Tables

Table 1: Descriptive Statistics for Realized Volatility, Quadratic Power Variation, and Jump Variables

Commodity	Variable	Obs	Mean	Std. Dev.	Min	Max
Panel A: Realized Volatility						
Crude Oil	$RV_{t,NAV}$	3,935	0.081	0.717	0.002	42.082
	$RV_{t,ETF}$	3,935	0.066	0.204	0.001	10.335
Gold	$RV_{t,NAV}$	3,935	0.012	0.017	0.001	0.327
	$RV_{t,ETF}$	3,935	0.034	1.259	0.001	78.988
Silver	$RV_{t,NAV}$	3,935	0.043	0.063	0.002	1.120
	$RV_{t,ETF}$	3,935	0.042	0.067	0.004	1.286
Natural Gas	$RV_{t,NAV}$	3,935	0.104	0.173	0.010	6.635
	$RV_{t,ETF}$	3,935	0.103	0.116	0.004	1.651
Panel B: Quadratic Power Variation						
Crude Oil	$QPV_{t,NAV}$	3,935	0.110	6.797	0.000	426.363
	$QPV_{t,ETF}$	3,935	0.003	0.121	0.000	7.295
Gold	$QPV_{t,NAV}$	3,935	0.000	0.000	0.000	0.007
	$QPV_{t,ETF}$	3,935	0.000	0.000	0.000	0.027
Silver	$QPV_{t,NAV}$	3,935	0.000	0.003	0.000	0.139
	$QPV_{t,ETF}$	3,935	0.000	0.001	0.000	0.043
Natural Gas	$QPV_{t,NAV}$	3,935	0.003	0.152	0.000	9.555
	$QPV_{t,ETF}$	3,935	0.001	0.030	0.000	1.881
Panel C: Jump Component						
Crude Oil	$J_{t,NAV}$	3,935	-0.028	6.132	0.000	8.941
	$J_{t,ETF}$	3,935	0.063	0.124	0.000	3.040
Gold	$J_{t,NAV}$	3,935	0.012	0.017	0.001	0.324
	$J_{t,ETF}$	3,935	0.034	1.259	0.001	78.981
Silver	$J_{t,NAV}$	3,935	0.042	0.061	0.002	1.094
	$J_{t,ETF}$	3,935	0.042	0.066	0.004	1.243
Natural Gas	$J_{t,NAV}$	3,935	0.101	0.209	0.000	6.634
	$J_{t,ETF}$	3,935	0.102	0.113	0.000	1.651

This table presents descriptive statistics for realized volatility (RV), quadratic power variation (QPV), and jump component (J) variables constructed using 5-minute price data. All values are expressed in percentages. NAV refers to net asset value prices, and ETF refers to exchange-traded fund prices. The sample period includes 3,935 daily observations for each commodity.

Table 2: Descriptive Statistics for Realized Volatility, Quadratic Power Variation, and Jump Variables (1-minute data)

Commodity	Variable	Obs	Mean	Std. Dev.	Min	Max
Panel A: Realized Volatility						
Crude Oil	$RV_{t,NAV}$	3,935	0.083	0.959	0.001	58.167
	$RV_{t,ETF}$	3,935	0.058	0.250	0.001	14.051
Gold	$RV_{t,NAV}$	3,935	0.012	0.018	0.001	0.302
	$RV_{t,ETF}$	3,935	0.031	1.259	0.001	78.986
Silver	$RV_{t,NAV}$	3,935	0.040	0.064	0.001	1.347
	$RV_{t,ETF}$	3,935	0.036	0.061	0.002	1.367
Natural Gas	$RV_{t,NAV}$	3,935	0.099	0.174	0.007	6.699
	$RV_{t,ETF}$	3,935	0.086	0.096	0.004	1.634
Panel B: Quadratic Power Variation						
Crude Oil	$QPV_{t,NAV}$	3,935	0.019	1.152	0.000	72.288
	$QPV_{t,ETF}$	3,935	0.004	0.191	0.000	11.936
Gold	$QPV_{t,NAV}$	3,935	0.000	0.000	0.000	0.004
	$QPV_{t,ETF}$	3,935	0.000	0.000	0.000	0.016
Silver	$QPV_{t,NAV}$	3,935	0.000	0.001	0.000	0.060
	$QPV_{t,ETF}$	3,935	0.000	0.001	0.000	0.025
Natural Gas	$QPV_{t,NAV}$	3,935	0.000	0.004	0.000	0.232
	$QPV_{t,ETF}$	3,935	0.000	0.001	0.000	0.039
Panel C: Jump Component						
Crude Oil	$J_{t,NAV}$	3,935	0.064	0.330	0.000	8.933
	$J_{t,ETF}$	3,935	0.055	0.112	0.001	3.172
Gold	$J_{t,NAV}$	3,935	0.012	0.018	0.001	0.300
	$J_{t,ETF}$	3,935	0.031	1.259	0.001	78.969
Silver	$J_{t,NAV}$	3,935	0.040	0.063	0.001	1.328
	$J_{t,ETF}$	3,935	0.036	0.060	0.002	1.344
Natural Gas	$J_{t,NAV}$	3,935	0.098	0.173	0.007	6.697
	$J_{t,ETF}$	3,935	0.086	0.095	0.004	1.634

This table presents descriptive statistics for realized volatility (RV), quadratic power variation (QPV), and jump component (J) variables constructed using 1-minute price data. All values are expressed in percentages. NAV refers to net asset value prices, and ETF refers to exchange-traded fund prices. The sample period includes 3,935 daily observations for each commodity.

Table 3: Descriptive Statistics for Realized Volatility, Quadratic Power Variation, and Jump Variables (30-minute data)

Commodity	Variable	Obs	Mean	Std. Dev.	Min	Max
Panel A: Realized Volatility						
Crude Oil	$RV_{t,NAV}$	3,935	0.073	0.459	0.001	23.817
	$RV_{t,ETF}$	3,935	0.052	0.176	0.000	8.995
Gold	$RV_{t,NAV}$	3,935	0.011	0.019	0.001	0.407
	$RV_{t,ETF}$	3,935	0.030	1.257	0.000	78.854
Silver	$RV_{t,NAV}$	3,935	0.039	0.069	0.001	1.701
	$RV_{t,ETF}$	3,935	0.033	0.060	0.001	1.618
Natural Gas	$RV_{t,NAV}$	3,935	0.093	0.176	0.004	6.829
	$RV_{t,ETF}$	3,935	0.077	0.093	0.002	1.668
Panel B: Quadratic Power Variation						
Crude Oil	$QPV_{t,NAV}$	3,935	0.002	0.067	0.000	4.036
	$QPV_{t,ETF}$	3,935	0.000	0.013	0.000	0.831
Gold	$QPV_{t,NAV}$	3,935	0.000	0.000	0.000	0.002
	$QPV_{t,ETF}$	3,935	0.000	0.000	0.000	0.002
Silver	$QPV_{t,NAV}$	3,935	0.000	0.001	0.000	0.050
	$QPV_{t,ETF}$	3,935	0.000	0.001	0.000	0.037
Natural Gas	$QPV_{t,NAV}$	3,935	0.000	0.001	0.000	0.044
	$QPV_{t,ETF}$	3,935	0.000	0.001	0.000	0.035
Panel C: Jump Component						
Crude Oil	$J_{t,NAV}$	3,935	0.072	0.401	0.001	19.781
	$J_{t,ETF}$	3,935	0.051	0.165	0.000	8.164
Gold	$J_{t,NAV}$	3,935	0.011	0.018	0.001	0.404
	$J_{t,ETF}$	3,935	0.030	1.257	0.000	78.852
Silver	$J_{t,NAV}$	3,935	0.038	0.068	0.001	1.665
	$J_{t,ETF}$	3,935	0.033	0.059	0.001	1.583
Natural Gas	$J_{t,NAV}$	3,935	0.093	0.175	0.004	6.823
	$J_{t,ETF}$	3,935	0.077	0.093	0.002	1.633

This table presents descriptive statistics for realized volatility (RV), quadratic power variation (QPV), and jump component (J) variables constructed using 30-minute price data. All values are expressed in percentages. NAV refers to net asset value prices, and ETF refers to exchange-traded fund prices. The sample period includes 3,935 daily observations for each commodity.

Table 4: HAR-X Model Estimates with 5-minute Realized Variance

	Crude Oil		**Gold**		**Silver**		**Natural Gas**	
	$RV_{t,NAV}$	$RV_{t,ETF}$	$RV_{t,NAV}$	$RV_{t,ETF}$	$RV_{t,NAV}$	$RV_{t,ETF}$	$RV_{t,NAV}$	$RV_{t,ETF}$
$RV_{t-1,NAV}$	0.288***	0.311***	0.253***	0.515***	0.345***	0.383***	0.092**	0.105***
	(0.000)	(0.000)	(0.000)	(0.000)	(0.000)	(0.000)	(0.000)	(0.000)
$\overline{RV}_{t-5,NAV}$	0.408***		0.338***		0.318***		0.393***	
	(0.000)		(0.000)		(0.000)		(0.000)	
$\overline{RV}_{t-22,NAV}$	0.144***		0.321***		0.271***		0.313***	
	(0.000)		(0.000)		(0.000)		(0.000)	
$RV_{t-1,ETF}$	0.111***	0.098***	0.021	−0.084*	−0.009	−0.015	0.126***	0.084***
	(0.000)	(0.000)	(0.158)	(0.062)	(0.612)	(0.464)	(0.000)	(0.000)
$\overline{RV}_{t-5,ETF}$		0.297***		0.270***		0.209***		0.431***
		(0.000)		(0.000)		(0.000)		(0.000)
$\overline{RV}_{t-22,ETF}$		0.227***		0.164***		0.342***		0.332***
		(0.000)		(0.000)		(0.000)		(0.000)
Observations	3,935	3,935	3,935	3,935	3,935	3,935	3,935	3,935

This table presents estimation results for the HAR-X model using 5-minute realized variance data. The dependent variables are the realized variances for NAV and ETF prices of each commodity. Standard errors are reported in parentheses. ***, **, and * denote statistical significance at the 1%, 5%, and 10% levels, respectively. RV_{t-1} represents the lagged daily realized variance, $\overline{RV}_{t-5}$ is the average of the past 5 days' realized variances, and $\overline{RV}_{t-22}$ is the average of the past 22 days' realized variances.

Table 5: HAR-X Model Estimates with 1-minute Realized Variance

	Crude Oil		Gold		Silver		Natural Gas	
	$RV_{t,NAV}$	$RV_{t,ETF}$	$RV_{t,NAV}$	$RV_{t,ETF}$	$RV_{t,NAV}$	$RV_{t,ETF}$	$RV_{t,NAV}$	$RV_{t,ETF}$
$RV_{t-1,NAV}$	0.371***	0.378***	0.331***	0.632***	0.404***	0.418***	0.121***	0.079***
	(0.000)	(0.000)	(0.000)	(0.000)	(0.000)	(0.000)	(0.000)	(0.000)
$\overline{RV}_{t-5,NAV}$	0.387***		0.329***		0.297***		0.386***	
	(0.000)		(0.000)		(0.000)		(0.000)	
$\overline{RV}_{t-22,NAV}$	0.109***		0.280***		0.226***		0.285***	
	(0.000)		(0.000)		(0.000)		(0.000)	
$RV_{t-1,ETF}$	0.089***	0.097***	−0.001	−0.059*	0.004	0.015	0.127***	0.124***
	(0.000)	(0.000)	(0.961)	(0.065)	(0.804)	(0.410)	(0.000)	(0.000)
$\overline{RV}_{t-5,ETF}$		0.272***		0.196***		0.206***		0.438***
		(0.000)		(0.000)		(0.000)		(0.000)
$\overline{RV}_{t-22,ETF}$		0.200***		0.113***		0.276***		0.318***
		(0.000)		(0.000)		(0.000)		(0.000)
Observations	3,935	3,935	3,935	3,935	3,935	3,935	3,935	3,935

This table presents estimation results for the HAR-X model using 1-minute realized variance data. The dependent variables are the realized variances for NAV and ETF prices of each commodity. Standard errors are reported in parentheses. ***, **, and * denote statistical significance at the 1%, 5%, and 10% levels, respectively. RV_{t-1} represents the lagged daily realized variance, $\overline{RV}_{t-5}$ is the average of the past 5 days' realized variances, and $\overline{RV}_{t-22}$ is the average of the past 22 days' realized variances.

Table 6: HAR-X Model Estimates with 30-minute Realized Variance

	Crude Oil		**Gold**		**Silver**		**Natural Gas**	
	$RV_{t,NAV}$	$RV_{t,ETF}$	$RV_{t,NAV}$	$RV_{t,ETF}$	$RV_{t,NAV}$	$RV_{t,ETF}$	$RV_{t,NAV}$	$RV_{t,ETF}$
$RV_{t-1,NAV}$	0.133***	0.200***	0.150***	0.387***	0.226***	0.277***	0.043	0.081***
	(0.000)	(0.000)	(0.000)	(0.000)	(0.000)	(0.000)	(0.121)	(0.000)
$\overline{RV}_{t-5,NAV}$	0.461***		0.335***		0.319***		0.399***	
	(0.000)		(0.000)		(0.000)		(0.000)	
$\overline{RV}_{t-22,NAV}$	0.243***		0.445***		0.394***		0.393***	
	(0.000)		(0.000)		(0.000)		(0.000)	
$RV_{t-1,ETF}$	0.103***	0.049	−0.015	−0.128**	−0.034	−0.075**	0.074**	0.012
	(0.000)	(0.149)	(0.476)	(0.019)	(0.140)	(0.013)	(0.030)	(0.662)
$\overline{RV}_{t-5,ETF}$		0.363***		0.332***		0.238***		0.405***
		(0.000)		(0.000)		(0.000)		(0.000)
$\overline{RV}_{t-22,ETF}$		0.319***		0.212***		0.460***		0.447***
		(0.000)		(0.000)		(0.000)		(0.000)
Observations	3,935	3,935	3,935	3,935	3,935	3,935	3,935	3,935

This table presents estimation results for the HAR-X model using 30-minute realized variance data. The dependent variables are the realized variances for NAV and ETF prices of each commodity. Standard errors are reported in parentheses. ***, **, and * denote statistical significance at the 1%, 5%, and 10% levels, respectively. RV_{t-1} represents the lagged daily realized variance, $\overline{RV}_{t-5}$ is the average of the past 5 days' realized variances, and $\overline{RV}_{t-22}$ is the average of the past 22 days' realized variances.

Table 7: HAR-CJ-X Model Estimates with 5-minute Realized Variance

	Crude Oil		Gold		Silver		Natural Gas	
	$RV_{t,NAV}$	$RV_{t,ETF}$	$RV_{t,NAV}$	$RV_{t,ETF}$	$RV_{t,NAV}$	$RV_{t,ETF}$	$RV_{t,NAV}$	$RV_{t,ETF}$
Panel A: Quadratic Power Variation								
$QPV_{t-1,NAV}$	0.049**	0.008	0.026	−0.001	−0.015	−0.026	0.065***	0.016
	(0.025)	(0.661)	(0.239)	(0.957)	(0.467)	(0.273)	(0.001)	(0.400)
$\overline{QPV}_{t-5,NAV}$	0.032		−0.027		−0.030		0.110***	
	(0.167)		(0.317)		(0.236)		(0.000)	
$\overline{QPV}_{t-22,NAV}$	−0.046***		−0.021		−0.005		0.044**	
	(0.007)		(0.341)		(0.793)		(0.018)	
$QPV_{t-1,ETF}$	0.001	0.043**	−0.015	−0.030	0.006	0.010	0.011	0.028*
	(0.969)	(0.038)	(0.545)	(0.248)	(0.779)	(0.686)	(0.620)	(0.088)
$\overline{QPV}_{t-5,ETF}$		0.017		−0.008		−0.003		0.062***
		(0.454)		(0.737)		(0.876)		(0.001)
$\overline{QPV}_{t-22,ETF}$		−0.040**		0.133***		0.006		0.038
		(0.043)		(0.000)		(0.763)		(0.137)
Panel B: Jump Component								
$J_{t-1,NAV}$	0.207***	0.280***	0.212***	0.491***	0.375***	0.431***	−0.003	0.057*
	(0.000)	(0.000)	(0.000)	(0.000)	(0.000)	(0.000)	(0.923)	(0.082)
$\overline{J}_{t-5,NAV}$	0.338***		0.407***		0.389***		0.220***	
	(0.000)		(0.000)		(0.000)		(0.000)	
$\overline{J}_{t-22,NAV}$	0.267***		0.354***		0.272***		0.213***	
	(0.000)		(0.000)		(0.000)		(0.000)	
$J_{t-1,ETF}$	0.094***	0.019	0.041	−0.023	−0.016	−0.030	0.044	0.039
	(0.000)	(0.473)	(0.156)	(0.497)	(0.527)	(0.291)	(0.190)	(0.195)
$\overline{J}_{t-5,ETF}$		0.264***		0.246***		0.214***		0.307***
		(0.000)		(0.000)		(0.000)		(0.000)
$\overline{J}_{t-22,ETF}$		0.329***		−0.014		0.327***		0.250***
		(0.000)		(0.631)		(0.000)		(0.000)
Observations	3,935	3,935	3,935	3,935	3,935	3,935	3,935	3,935

This table presents estimation results for the HAR-CJ-X model using 5-minute realized variance data. The model incorporates both continuous (quadratic power variation, QPV) and jump (J) components. The dependent variables are the realized variances for NAV and ETF prices of each commodity. Standard errors are reported in parentheses. ***, **, and * denote statistical significance at the 1%, 5%, and 10% levels, respectively. QPV_{t-1} and J_{t-1} represent the lagged daily components, while $\overline{QPV}_{t-5}$, $\overline{J}_{t-5}$, $\overline{QPV}_{t-22}$, and $\overline{J}_{t-22}$ are the corresponding weekly and monthly averages.

Table 8: HAR-CJ-X Model Estimates with 1-minute Realized Variance

	Crude Oil		**Gold**		**Silver**		**Natural Gas**	
	$RV_{t,NAV}$	$RV_{t,ETF}$	$RV_{t,NAV}$	$RV_{t,ETF}$	$RV_{t,NAV}$	$RV_{t,ETF}$	$RV_{t,NAV}$	$RV_{t,ETF}$
Panel A: Quadratic Power Variation								
$QPV_{t-1,NAV}$	0.036	−0.019	−0.033*	−0.123***	−0.041**	−0.065***	0.008	−0.002
	(0.246)	(0.525)	(0.096)	(0.000)	(0.039)	(0.002)	(0.773)	(0.920)
$\overline{QPV}_{t-5,NAV}$	−0.021		−0.076***		−0.068***		0.116***	
	(0.444)		(0.004)		(0.009)		(0.000)	
$\overline{QPV}_{t-22,NAV}$	−0.031		−0.001		0.009		−0.040**	
	(0.309)		(0.976)		(0.716)		(0.046)	
$QPV_{t-1,ETF}$	−0.011	0.009	−0.020*	−0.032*	−0.011	−0.014	−0.011	−0.021*
	(0.665)	(0.698)	(0.062)	(0.089)	(0.617)	(0.514)	(0.671)	(0.089)
$\overline{QPV}_{t-5,ETF}$		−0.014		0.016		0.003		0.016
		(0.591)		(0.566)		(0.895)		(0.554)
$\overline{QPV}_{t-22,ETF}$		−0.024**		0.060***		−0.017		−0.014
		(0.036)		(0.003)		(0.463)		(0.617)
Panel B: Jump Component								
$J_{t-1,NAV}$	0.306***	0.432***	0.426***	0.892***	0.510***	0.578***	0.092*	0.090***
	(0.000)	(0.000)	(0.000)	(0.000)	(0.000)	(0.000)	(0.075)	(0.000)
$\bar{J}_{t-5,NAV}$	0.435***		0.509***		0.468***		0.219***	
	(0.000)		(0.000)		(0.000)		(0.000)	
$\bar{J}_{t-22,NAV}$	0.190***		0.234***		0.161***		0.346***	
	(0.000)		(0.000)		(0.000)		(0.000)	
$J_{t-1,ETF}$	0.096***	0.077**	0.031	0.011	0.028	0.051	0.128***	0.166***
	(0.000)	(0.019)	(0.290)	(0.689)	(0.313)	(0.106)	(0.000)	(0.000)
$\bar{J}_{t-5,ETF}$		0.300***		0.132**		0.184***		0.401***
		(0.000)		(0.023)		(0.000)		(0.000)
$\bar{J}_{t-22,ETF}$		0.250***		0.028		0.295***		0.350***
		(0.000)		(0.455)		(0.000)		(0.000)
Observations	3,935	3,935	3,935	3,935	3,935	3,935	3,935	3,935

This table presents estimation results for the HAR-CJ-X model using 1-minute realized variance data. The model incorporates both continuous (quadratic power variation, QPV) and jump (J) components. The dependent variables are the realized variances for NAV and ETF prices of each commodity. Standard errors are reported in parentheses. ***, **, and * denote statistical significance at the 1%, 5%, and 10% levels, respectively. QPV_{t-1} and J_{t-1} represent the lagged daily components, while $\overline{QPV}_{t-5}$, $\bar{J}_{t-5}$, $\overline{QPV}_{t-22}$, and $\bar{J}_{t-22}$ are the corresponding weekly and monthly averages.

Table 9: HAR-CJ-X Model Estimates with 30-minute Realized Variance

	Crude Oil		Gold		Silver		Natural Gas	
	$RV_{t,NAV}$	$RV_{t,ETF}$	$RV_{t,NAV}$	$RV_{t,ETF}$	$RV_{t,NAV}$	$RV_{t,ETF}$	$RV_{t,NAV}$	$RV_{t,ETF}$
Panel A: Quadratic Power Variation								
$QPV_{t-1,NAV}$	0.019	−0.026	0.058***	0.067***	0.013	0.033	0.057***	0.027
	(0.535)	(0.421)	(0.005)	(0.003)	(0.596)	(0.235)	(0.008)	(0.278)
$\overline{QPV}_{t-5,NAV}$	0.029		−0.051**		−0.008		0.114***	
	(0.375)		(0.044)		(0.779)		(0.000)	
$\overline{QPV}_{t-22,NAV}$	−0.001		0.001		−0.045*		0.156***	
	(0.975)		(0.977)		(0.098)		(0.000)	
$QPV_{t-1,ETF}$	−0.010	0.015	−0.018	−0.027	−0.006	0.001	−0.014	0.001
	(0.683)	(0.562)	(0.489)	(0.313)	(0.799)	(0.984)	(0.575)	(0.972)
$\overline{QPV}_{t-5,ETF}$		0.055**		−0.017		−0.001		0.079***
		(0.033)		(0.517)		(0.966)		(0.001)
$\overline{QPV}_{t-22,ETF}$		0.016		0.234***		−0.035		0.168***
		(0.517)		(0.000)		(0.191)		(0.000)
Panel B: Jump Component								
$J_{t-1,NAV}$	0.110**	0.221***	0.054	0.206***	0.201***	0.216***	−0.006	0.027
	(0.019)	(0.000)	(0.190)	(0.000)	(0.000)	(0.000)	(0.870)	(0.381)
$\overline{J}_{t-5,NAV}$	0.403***		0.436***		0.339***		0.204***	
	(0.000)		(0.000)		(0.000)		(0.000)	
$\overline{J}_{t-22,NAV}$	0.248***		0.440***		0.489***		0.089	
	(0.000)		(0.000)		(0.000)		(0.123)	
$J_{t-1,ETF}$	0.110***	0.043	0.009	−0.059	−0.023	−0.080*	0.016	0.007
	(0.000)	(0.181)	(0.772)	(0.183)	(0.428)	(0.077)	(0.608)	(0.823)
$\overline{J}_{t-5,ETF}$		0.259***		0.274***		0.241***		0.243***
		(0.000)		(0.000)		(0.000)		(0.000)
$\overline{J}_{t-22,ETF}$		0.283***		−0.082*		0.532***		0.088
		(0.000)		(0.058)		(0.000)		(0.224)
Observations	3,935	3,935	3,935	3,935	3,935	3,935	3,935	3,935

This table presents estimation results for the HAR-CJ-X model using 30-minute realized variance data. The model incorporates both continuous (quadratic power variation, QPV) and jump (J) components. The dependent variables are the realized variances for NAV and ETF prices of each commodity. Standard errors are reported in parentheses. ***, **, and * denote statistical significance at the 1%, 5%, and 10% levels, respectively. QPV_{t-1} and J_{t-1} represent the lagged daily components, while $\overline{QPV}_{t-5}$, $\overline{J}_{t-5}$, $\overline{QPV}_{t-22}$, and $\overline{J}_{t-22}$ are the corresponding weekly and monthly averages.

Table 10: Bayesian Vector Autoregression Results: USO ETF and Net Asset Value

Variable	**Panel A:** $\log(RV_{t,NAV})$					
	Mean	Std. Dev.	MCSE	Median	95% Credible Interval	
					Lower	Upper
$\log(RV_{t-1,NAV})$	0.570	0.024	0.000	0.570	0.524	0.617
$\log(RV_{t-2,NAV})$	0.261	0.021	0.000	0.261	0.221	0.300
$\log(RV_{t-1,ETF})$	0.074	0.020	0.000	0.074	0.034	0.113
$\log(RV_{t-2,ETF})$	0.016	0.018	0.000	0.016	-0.019	0.051
	Panel B: $\log(RV_{t,ETF})$					
Variable	Mean	Std. Dev.	MCSE	Median	95% Credible Interval	
					Lower	Upper
$\log(RV_{t-1,NAV})$	0.286	0.028	0.000	0.286	0.231	0.343
$\log(RV_{t-2,NAV})$	0.193	0.025	0.000	0.193	0.144	0.241
$\log(RV_{t-1,ETF})$	0.294	0.024	0.000	0.294	0.246	0.342
$\log(RV_{t-2,ETF})$	0.106	0.022	0.000	0.106	0.064	0.148

This table presents posterior statistics from a Bayesian Vector Autoregression (VAR) model analyzing the relationship between the USO ETF and its Net Asset Value (NAV). Panel A shows results for the NAV equation, while Panel B shows results for the ETF equation. The model includes two lags of both log realized variances. Mean represents the posterior mean, Std. Dev. is the posterior standard deviation, MCSE is the Monte Carlo standard error, Median is the posterior median, and the 95% credible interval provides the range of plausible parameter values. All realized variance measures are constructed using 5-minute price data.

Table 11: Bayesian Vector Autoregression Results: GLD ETF and Net Asset Value

Variable	Mean	Std. Dev.	MCSE	Median	95% Credible Interval Lower	95% Credible Interval Upper
Panel A: $\log(RV_{t,NAV})$						
$\log(RV_{t-1,NAV})$	0.551	0.027	0.000	0.551	0.498	0.603
$\log(RV_{t-2,NAV})$	0.248	0.023	0.000	0.248	0.203	0.293
$\log(RV_{t-1,ETF})$	−0.010	0.023	0.000	−0.010	−0.055	0.034
$\log(RV_{t-2,ETF})$	0.038	0.019	0.000	0.038	0.000	0.076
Panel B: $\log(RV_{t,ETF})$						
$\log(RV_{t-1,NAV})$	0.349	0.033	0.000	0.348	0.285	0.413
$\log(RV_{t-2,NAV})$	0.276	0.028	0.000	0.276	0.222	0.331
$\log(RV_{t-1,ETF})$	0.155	0.028	0.000	0.155	0.100	0.208
$\log(RV_{t-2,ETF})$	0.048	0.023	0.000	0.048	0.003	0.095

This table presents posterior statistics from a Bayesian Vector Autoregression (VAR) model analyzing the relationship between the GLD ETF and its Net Asset Value (NAV). Panel A shows results for the NAV equation, while Panel B shows results for the ETF equation. The model includes two lags of both log realized variances. Mean represents the posterior mean, Std. Dev. is the posterior standard deviation, MCSE is the Monte Carlo standard error, Median is the posterior median, and the 95% credible interval provides the range of plausible parameter values. All realized variance measures are constructed using 5-minute price data.

Table 12: Bayesian Vector Autoregression Results: SLV ETF and Net Asset Value

Panel A: $\log(RV_{t,NAV})$

Variable	Mean	Std. Dev.	MCSE	Median	95% Credible Interval	
					Lower	Upper
$\log(RV_{t-1,NAV})$	0.619	0.028	0.000	0.619	0.563	0.674
$\log(RV_{t-2,NAV})$	0.214	0.024	0.000	0.214	0.168	0.261
$\log(RV_{t-1,ETF})$	-0.045	0.025	0.000	-0.045	-0.093	0.005
$\log(RV_{t-2,ETF})$	0.058	0.021	0.000	0.058	0.018	0.100

Panel B: $\log(RV_{t,ETF})$

Variable	Mean	Std. Dev.	MCSE	Median	95% Credible Interval	
					Lower	Upper
$\log(RV_{t-1,NAV})$	0.376	0.033	0.000	0.377	0.310	0.440
$\log(RV_{t-2,NAV})$	0.202	0.028	0.000	0.202	0.147	0.256
$\log(RV_{t-1,ETF})$	0.179	0.029	0.000	0.179	0.123	0.236
$\log(RV_{t-2,ETF})$	0.078	0.024	0.000	0.078	0.031	0.126

This table presents posterior statistics from a Bayesian Vector Autoregression (VAR) model analyzing the relationship between the SLV ETF and its Net Asset Value (NAV). Panel A shows results for the NAV equation, while Panel B shows results for the ETF equation. The model includes two lags of both log realized variances. Mean represents the posterior mean, Std. Dev. is the posterior standard deviation, MCSE is the Monte Carlo standard error, Median is the posterior median, and the 95% credible interval provides the range of plausible parameter values. All realized variance measures are constructed using 5-minute price data.

Table 13: Bayesian Vector Autoregression Results: UNG ETF and Net Asset Value

Variable	Mean	Std. Dev.	MCSE	Median	95% Credible Interval Lower	95% Credible Interval Upper
Panel A: $\log(RV_{t,NAV})$						
$\log(RV_{t-1,NAV})$	0.392	0.022	0.000	0.392	0.349	0.437
$\log(RV_{t-2,NAV})$	0.231	0.020	0.000	0.231	0.192	0.272
$\log(RV_{t-1,ETF})$	0.080	0.021	0.000	0.080	0.038	0.121
$\log(RV_{t-2,ETF})$	0.157	0.019	0.000	0.157	0.119	0.194
Panel B: $\log(RV_{t,ETF})$						
$\log(RV_{t-1,NAV})$	0.130	0.024	0.000	0.130	0.083	0.177
$\log(RV_{t-2,NAV})$	0.165	0.022	0.000	0.165	0.124	0.208
$\log(RV_{t-1,ETF})$	0.339	0.023	0.000	0.339	0.294	0.383
$\log(RV_{t-2,ETF})$	0.240	0.020	0.000	0.240	0.200	0.280

This table presents posterior statistics from a Bayesian Vector Autoregression (VAR) model analyzing the relationship between the UNG ETF and its Net Asset Value (NAV). Panel A shows results for the NAV equation, while Panel B shows results for the ETF equation. The model includes two lags of both log realized variances. Mean represents the posterior mean, Std. Dev. is the posterior standard deviation, MCSE is the Monte Carlo standard error, Median is the posterior median, and the 95% credible interval provides the range of plausible parameter values. All realized variance measures are constructed using 5-minute price data.

7 Figures

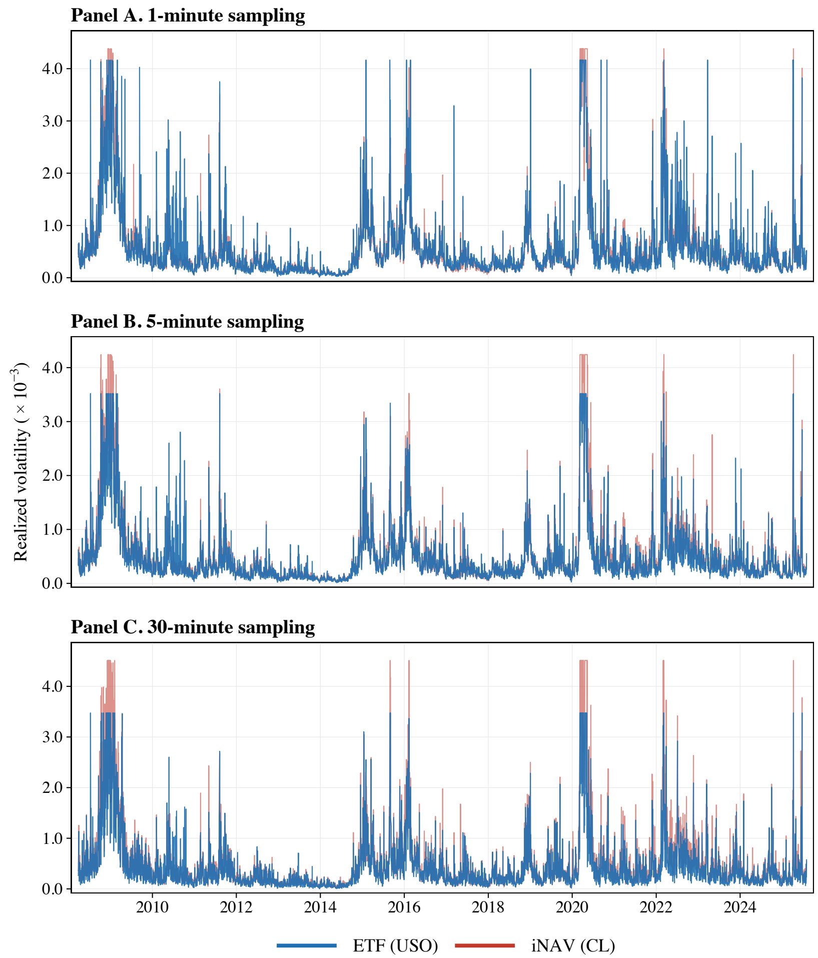

Figure 1: Realized volatility of the Crude Oil ETF and its iNAV. The figure plots daily realized volatility (sum of squared intraday log returns, $\times 10^{-3}$) for the USO ETF (blue) and its iNAV, proxied by the CL futures contract (red), from 2008-03-27 to 2025-08-01. Panels A, B, and C use returns sampled at the 1-minute, 5-minute, and 30-minute frequencies, respectively. For readability, each series is winsorized at its 99th percentile within each panel.

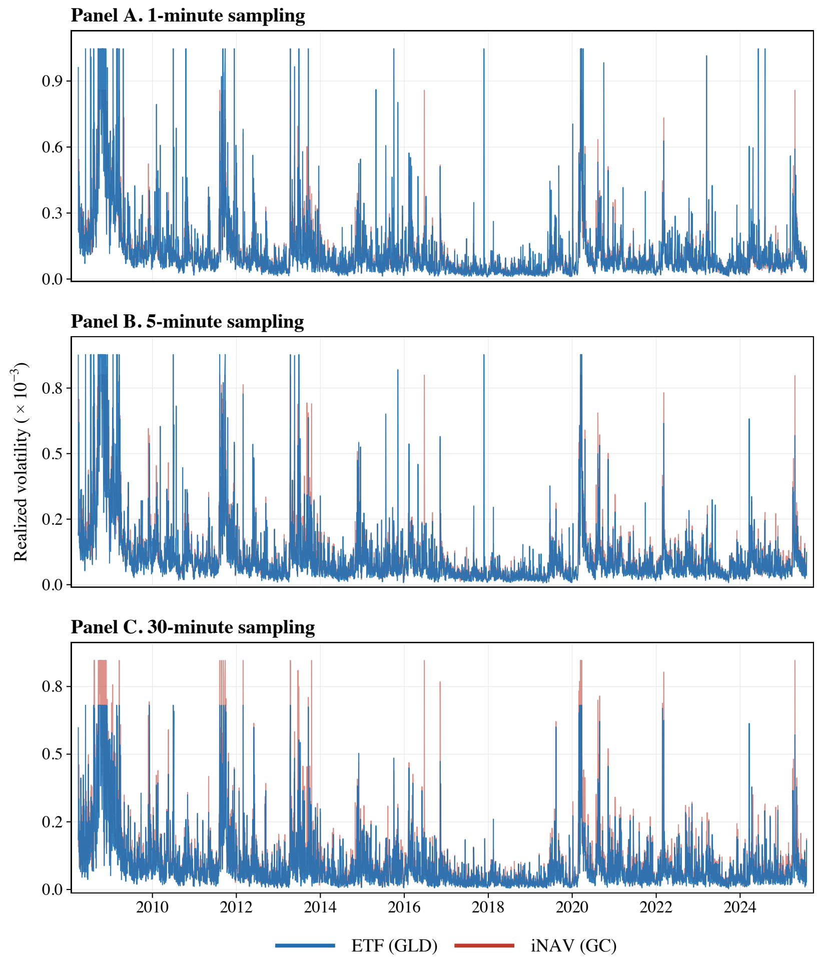

Figure 2: Realized volatility of the Gold ETF and its iNAV. The figure plots daily realized volatility (sum of squared intraday log returns, $\times 10^{-3}$) for the GLD ETF (blue) and its iNAV, proxied by the GC futures contract (red), from 2008-03-27 to 2025-08-01. Panels A, B, and C use returns sampled at the 1-minute, 5-minute, and 30-minute frequencies, respectively. For readability, each series is winsorized at its 99th percentile within each panel.

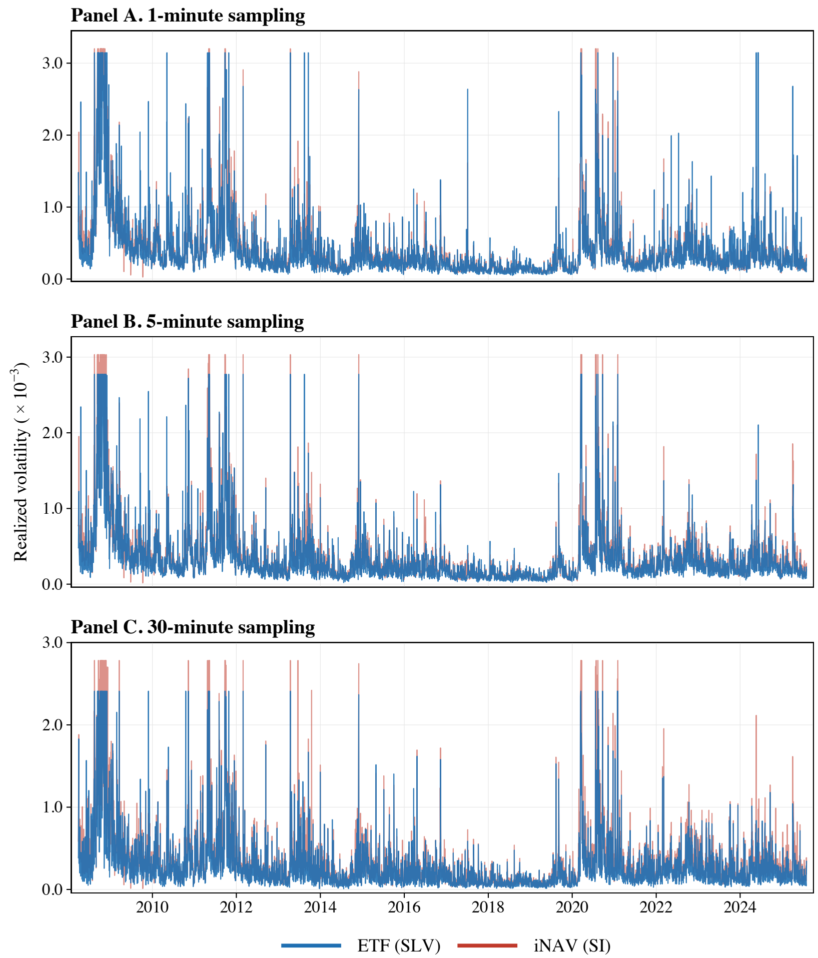

Figure 3: Realized volatility of the Silver ETF and its iNAV. The figure plots daily realized volatility (sum of squared intraday log returns, $\times 10^{-3}$) for the SLV ETF (blue) and its iNAV, proxied by the SI futures contract (red), from 2008-03-27 to 2025-08-01. Panels A, B, and C use returns sampled at the 1-minute, 5-minute, and 30-minute frequencies, respectively. For readability, each series is winsorized at its 99th percentile within each panel.

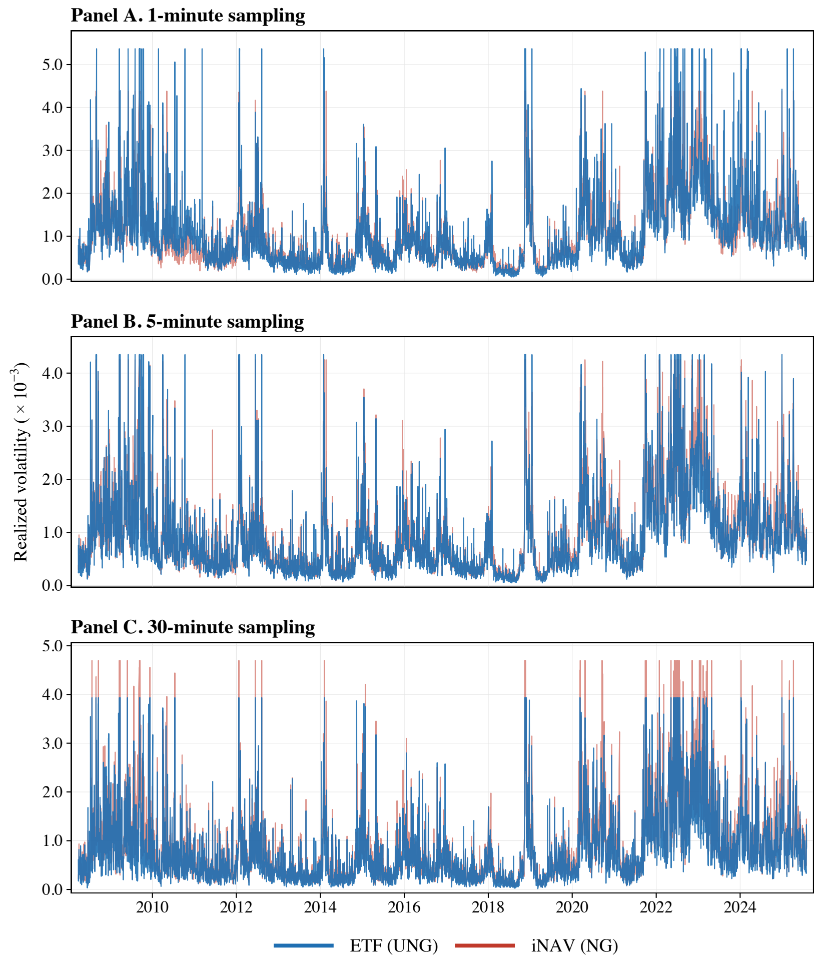

Figure 4: Realized volatility of the Natural Gas ETF and its iNAV. The figure plots daily realized volatility (sum of squared intraday log returns, $\times 10^{-3}$) for the UNG ETF (blue) and its iNAV, proxied by the NG futures contract (red), from 2008-03-27 to 2025-08-01. Panels A, B, and C use returns sampled at the 1-minute, 5-minute, and 30-minute frequencies, respectively. For readability, each series is winsorized at its 99th percentile within each panel.

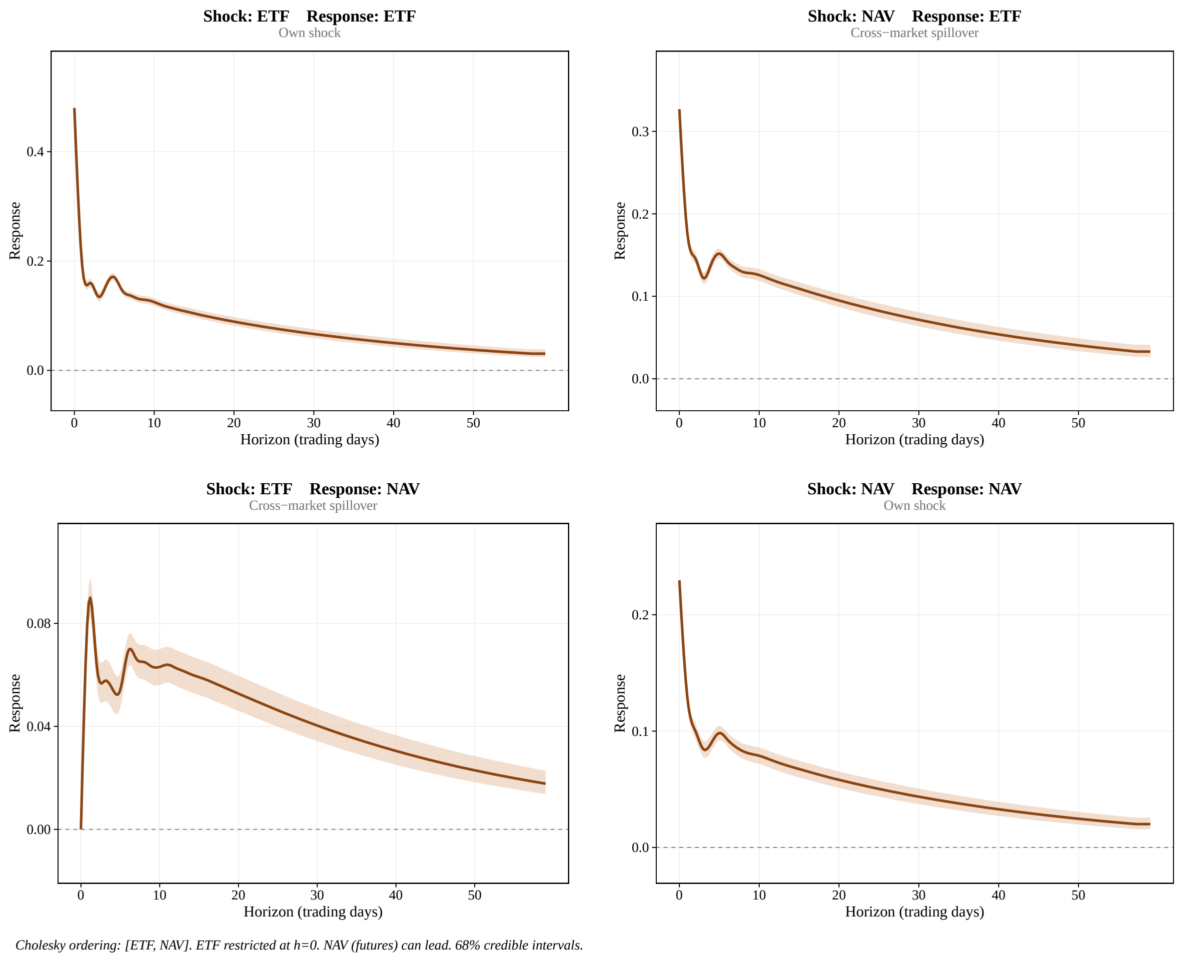

Figure 5: Impulse Response Functions (IRF) for USO ETF and Crude Oil (CL) iNAV Volatility. Bayesian VAR impulse responses showing fast shock absorption with systematic asymmetry: iNAV shocks cause large and persistent responses in ETF volatility while ETF shocks generate smaller and more transitory effects on iNAV, validating bidirectional but asymmetric transmission in crude oil markets.

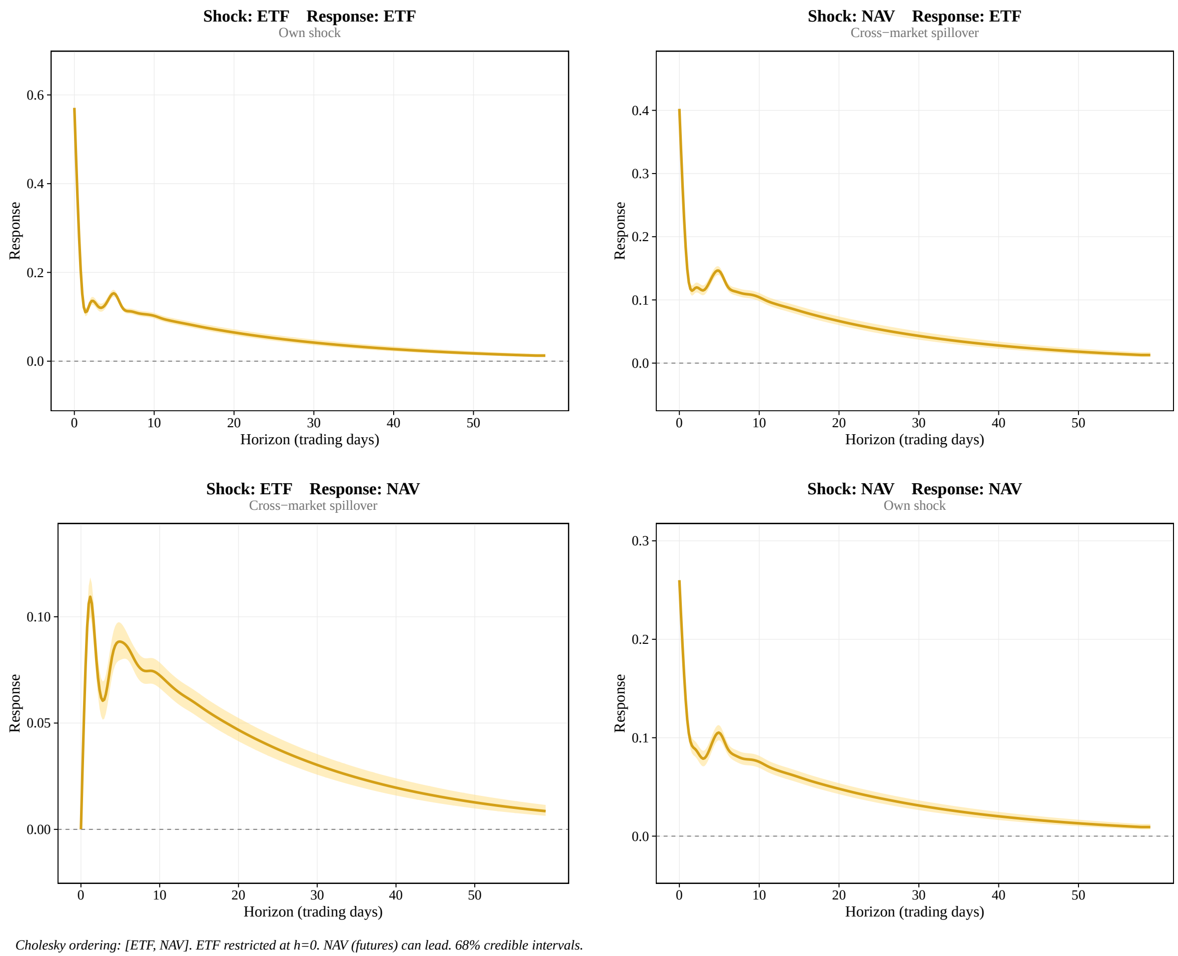

Figure 6: Impulse Response Functions (IRF) for GLD ETF and Gold (GC) iNAV Volatility. Bayesian VAR impulse responses exhibiting the most pronounced asymmetries: iNAV shocks create large and persistent responses in ETF volatility that decay smoothly, while ETF shocks generate negligible responses in iNAV, providing strong dynamic evidence for unidirectional transmission in gold markets.

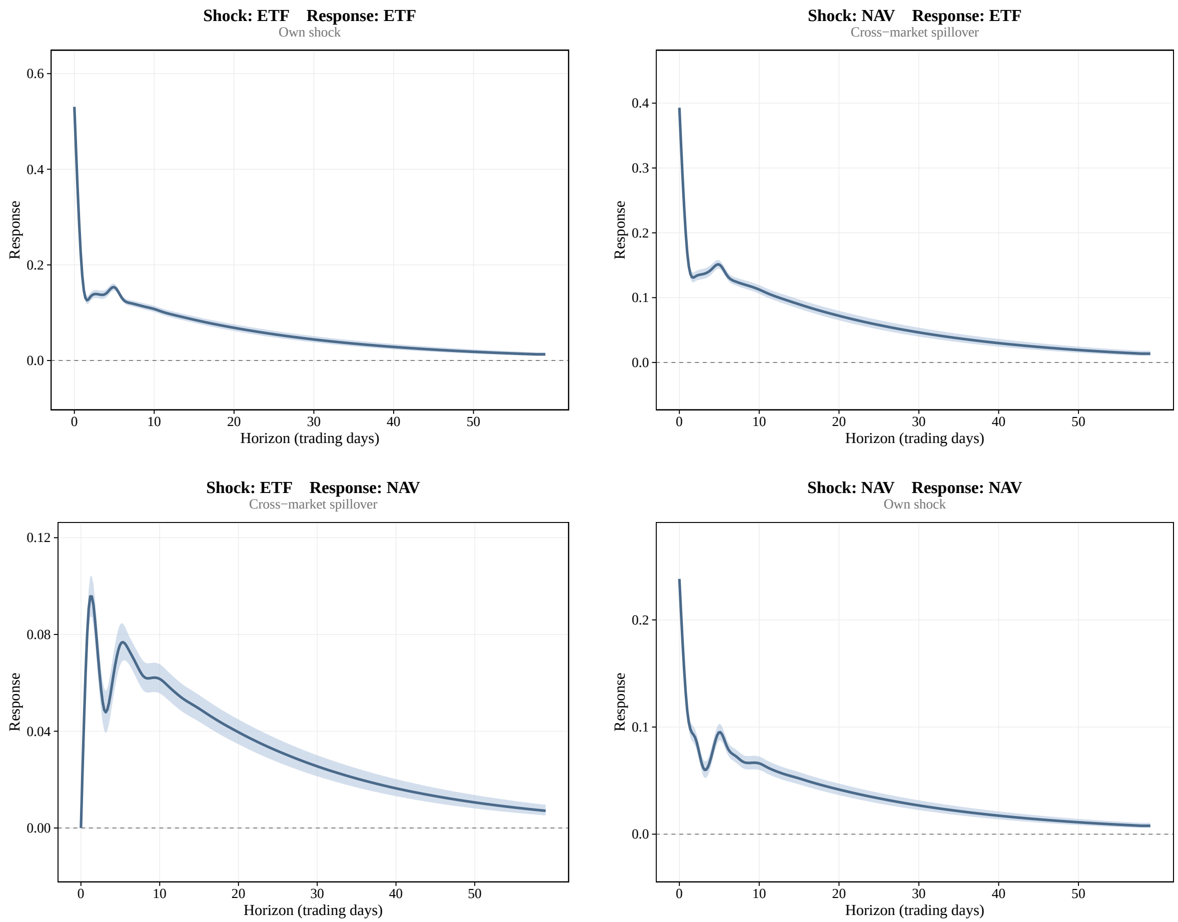

Cholesky ordering: [ETF, NAV]. ETF restricted at h=0. NAV (futures) can lead. 68% credible intervals.

Figure 7: Impulse Response Functions (IRF) for SLV ETF and Silver (SI) iNAV Volatility. Bayesian VAR impulse responses preserving the gold market's asymmetric structure but with qualitatively richer adjustment dynamics and greater variability, reflecting silver's dual function as both an industrial and a precious metal.

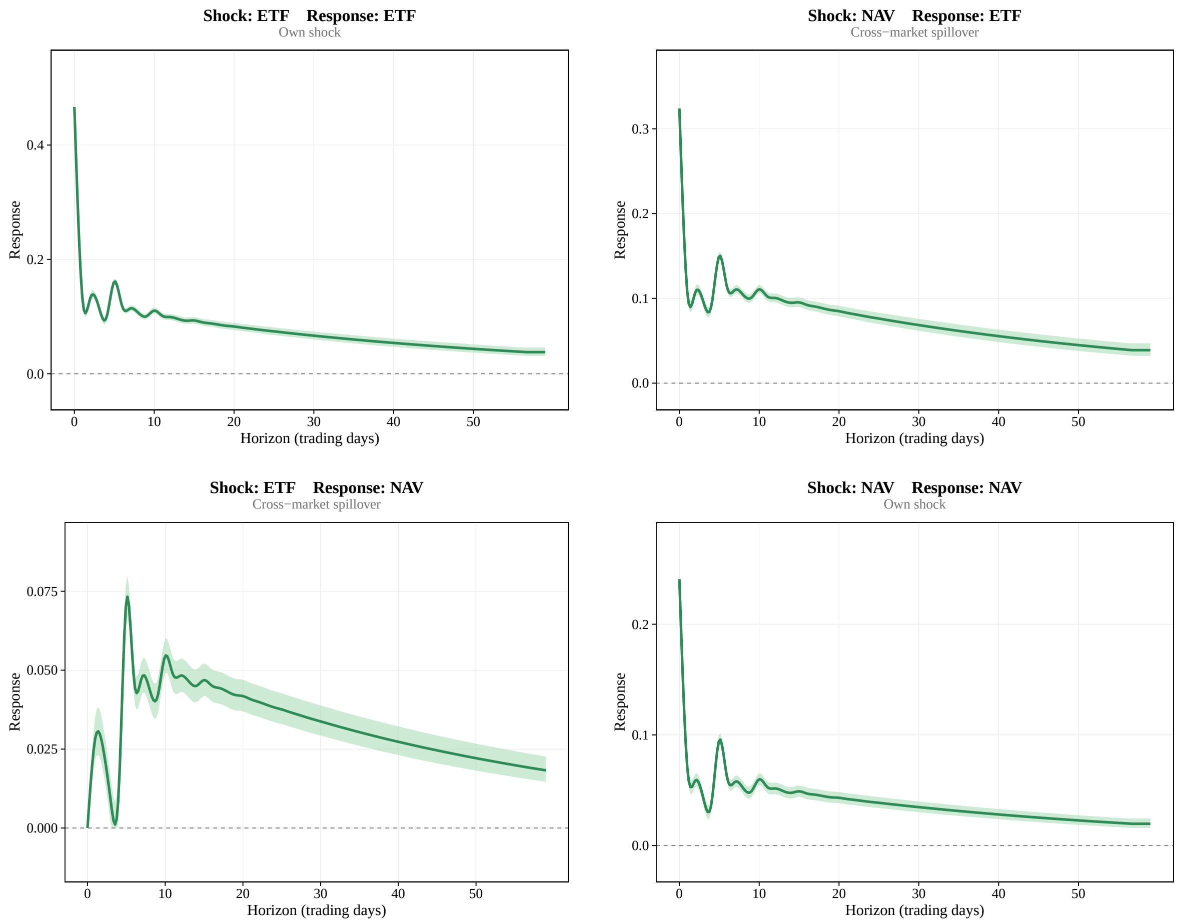

Cholesky ordering: [ETF, NAV]. ETF restricted at h=0. NAV (futures) can lead. 68% credible intervals.

Figure 8: Impulse Response Functions (IRF) for UNG ETF and Natural Gas (NG) iNAV Volatility. Bayesian VAR impulse responses exhibiting the most elaborate structures with large responses in both directions, delayed peaks, and periodic behavior, substantiating bidirectional transmission involving numerous channels and horizons in natural gas markets.